In vitro test of a potential hypoxic radiosensitizer

by

Yaowen Mei

A thesis

presented to the University of Waterloo

in fulfilment of the

thesis requirement for the degree of

Master of Science

in

Physics

Waterloo, Ontario, Canada, 2016

Author’s Declaration

I hereby declare that I am the sole author of this thesis. This is a true copy of the thesis, including any required final revisions, as accepted by my examiners.

I understand that my thesis may be made electronically available to the public

.

Abstract

Oxygen has long been known as a potent radiosensitizer that can enhance the cell killing effects in aerobic cells, while pruned vasculatures and lack of oxygen in the microenvironment of tumor can cause resistance to radiotherapy of cancer. Paradoxically, hypoxia also provides an attractive therapeutic target as it only occurs in solid tumors; hypoxia-activated radiosensitizers may be designed and synthesized with therapeutic selectivity on tumor cells.

Directed by our previous femotomedicine (FMD) mechanistic research, our group has recently discovered a FMD compound that can react with pre-solvated electron (e_{pre}^-) to increase the radiosensitivity in tumor tissues but relatively spare normal tissues. In this thesis work, the *in vitro* selective radiosensitivity of the FMD compound against hypoxic cancer cells was evaluated through the steady-state absorption spectrum analysis, the immunofluorescence assay, and the clonogenic assay. The results demonstrated that the FMD compound is an effective radiosensitizer in the hypoxic environment (radio enhancement ratio $=1.42 \pm 0.05$), and the potency of the radiosensitizing effect of the FMD compound in the oxic (normal) environment will be limited due to the competing attachments of pre-solvated electrons with the FMD molecules and molecular oxygens. The revealing of the underlying mechanism of the FMD compound's radiosensitizing effect provides new insight into the design of novel hypoxia-activated radiosensitizers.

Acknowledgements

I wish to express my sincere gratitude to my supervisor Dr. Qing-Bin Lu, for his constant guidance and support over the last two years, his prompt inspiration and timely suggestions helped me successfully carried out this project. I would also like to thank Dr Bae-Yeun Ha. and Dr Anton Burkov, Dr Ernest Osei for serving on my committee.

I am extremely thankful to our group members, Qinrong Zhang, Chun-Rong Wang, Wei Hong, Ning Ou, and Jenny Warrington for their meaningful assistance and comprehensive advice.

This project would have not been accomplished without the care and encouragement from my family and my girlfriend, Shuo Chen. Their love helped me resist the pressure and become a stronger person.

Last of all, I would like to give my special thanks to my friends: Chai Yu, Wei Cui, Jingfei Yao, and Shipei Zhu, who helped me directly or indirectly in completion of my research. I will never forget all of their kindness.

Dedication

To My Parents

Table of Contents

List of Tables

List of Figures

Chapter 1 Introduction

1.1 Cancer and cancer therapy

Cancer are the most challenging diseases in the world with high morbidity and mortality. In the year of 2016, more than 1.68 million people are projected to be diagnosed as cancer patients, and 595,690 people are estimated to be killed by cancer in the United States[1]. Based on a global survey from the World Health Organization in 2012[2], lung, prostate and colorectum were the three sites with the highest tendency to be diagnosed of cancer among men; meanwhile, among women, the three most common cancer incident sites were breasts, colorectum and lung. For both genders, lung, breasts and colorectum were the leading sites with the highest cancer incidence rates, at 12.9%, 11.9% and 9.7% of the total study population, respectively. They accounted for more than one third of the worldwide cancer burden[3].

From 2009 to 2016, more than ninety oncologic drugs were approved by the US Food and Drug Administration (FDA)[4]–[9]. With tremendous efforts of cancer researchers, several therapeutic methods for cancer have been established, such as 1) surgery, 2) radiotherapy, 3) chemotherapy, 4) photodynamic therapy (PDT), 5) hormones, etc. Surgery is the dominant choice of treatment after being diagnosed, and it is often combined with chemotherapy, radiotherapy, and photodynamic therapy. Radiotherapy, an alternative to surgery, is to use ionizing radiation to control or locally remove malignant cells. Generally, more than two

thirds of cancer patients will receive radiotherapy as a part of their treatment plan[10]. Chemotherapy is to use cytotoxic and cytostatic agents to kill malignant cells. This treatment is largely used for palliative in the advanced tumors which cannot be readily treated by surgery and radiation. Among all these therapeutics, surgery and radiotherapy are the two dominant curative treatments for cancer[11], but all the therapeutics can be involved for palliation[12]. However, so far, only a few radiosensitizing agents have been eventually approved by the FDA. Therefore, effective radiosensitizer， especially the one with selectivity that can spare normal tissue but remove the malignancy, should be a desired weapon in the battle against cancer. If it succeeds, these novel radiosensitizers will contribute considerably to human health and the lives of cancer patients.

1.2 Radiation therapy

The objective of radiation therapy is to use high energy radiation to cure or control cancer, or to reduce cancer symptoms. The amount of energy released by a radiation flux over its unit track length is defined as **linear energy transfer** (LET):

$$\text{LET}=dE/dx \quad , \qquad \textit{Eq. 1-1}$$

Where *dE* is the energy transferred to the medium by the radiation source while traversing a unit distance *dx*. For neutrons, α particles, and other heavy charged particles, as large amount of energy is deposited along the track, these types of radiations are called high linear energy transfer (High-LET) radiations. For radiations like X-Rays and γ-Rays, as less amount of energy is deposited per unit length and the ionizing events spread in wide spatial ranges, these kinds of radiation are called low linear energy transfer (Low-LET) radiations.

As DNA regulates a cell's activity and contains the information for a cell to replicate itself, damages to DNA will alter cell function and result in cell death. In radiation therapy, the most important target is the DNA in the cell. When the radiation-induced DNA damage cannot be repaired instantly or is improperly repaired, these DNA damages may lead to mutations, apoptosis, necrosis, and eventually the cell may lose the ability of proliferation. During ionizing radiation, there are two types of actions related to DNA damage will take place: direct and indirect action (see Figure 1-1). Direct action involves when the ionizing particle directly deposits its energy to ionize the genome; indirect action occurs when the

medium (predominantly water) absorbs most of the radiation energy and forms free radicals which produce further DNA damage[13]. By comparing the yield of γ-ray induced DNA strand breaks under aqueous and dry conditions at 25 ℃, it was shown that for Low-LET radiation, indirect actions can produce several orders of magnitude more DNA damages than direct actions[14].

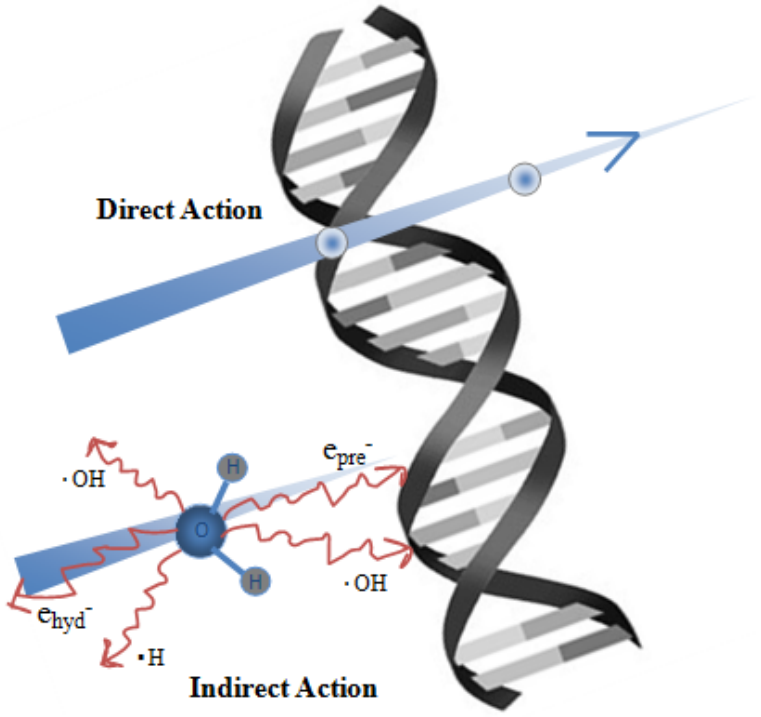

Figure 1-1. The schematic diagram illustrating the direct action and the indirect action when DNA is exposed to ionizing radiation. In the direct action, the radiation energy is directly deposited to DNA to produce chemical bond breaks. In the indirect action, the majority of the radiation energy is absorbed by surrounding water molecules, and DNA damages are indirectly produced via free radicals and reactive molecules which are formed by water radiolysis. For Low-LET radiation (like x-rays, and γ-rays), indirect action is predominant, and produces more DNA damages than direct action.

At the cellular level, the principal target for ionizing radiation (IR) is the cells' DNA. However, radiation kills both normal cells and abnormal cancer cells along its track

(especially for Low-LET radiations). The most important challenge in radiation therapy is minimizing the radiation-induced damage to the adjacent health tissue while maximizing the radiation killing efficiency to the cancer cells[15]. The response of a tissue to radiation depends on the types of the irradiated cells, the microenvironment of the irradiated cells, and also different cell cycle phases the cells are in. The cells with high reproductive activity are more sensitive to radiation. Generally, the cells in the quiescent G_0 or in the S phase show more resistance to radiation than the cells in M phase. The cells with high oxygen concentration are also more sensitive to radiation than the hypoxic tumor tissue (mechanism will be discussed in the following section). In radiation therapy, in order to minimize the damage to the adjacent and the overlying normal tissue and to reoxygenate the hypoxic tumor tissue, the radiation doses are often divided into many small fractions and given to patients over one to two months at a regular interval. Different fraction patterns, such as accelerated fractionation, hyper-fractionation and hypo-fractionation, are given to different patients depending on the severity and location of their tumors. Therefore, radiosensitizers, which can mimic the mechanism of oxygen and have natural selectivity that can sensitize the tumor tissue but spare the normal tissues and make the tumor to be cured by a large single dose instead of fraction doses, would greatly benefit the current concept of radiation therapy[16].

1.3 Water radiolysis

Radiation energy is absorbed by the components of the irradiated substance approximately proportionally to the mass of different components. When a cancer cell is irradiated, as cell is an aqueous system and water molecules make up to more than 70% of its cellular mass[17], water molecules will absorb most of the energy of the radiation flux. Consequently, the absorbed energy will lead to either excitation (Eq. 1-2) or ionization (Eq. 1-3) of these water molecules[18]:

$$H_2O \xrightarrow{Excitation} H_2O^* \qquad \textit{Eq. 1-2}$$

$$H_2O \xrightarrow{Ionization} H_2O^+ + e^- \qquad \textit{Eq. 1-3}$$

For the excited water molecules, the majority of the them do not dissociate, but just return back to the ground state (Eq. 1-4); while, only a small portion of them dissociate into hydrogen atoms and hydroxyl radicals (Eq. 1-5).

$$H_2O^* \longrightarrow H_2O \qquad \textit{Eq. 1-4}$$

$$H_2O^* \longrightarrow H^\bullet + HO^\bullet \qquad \textit{Eq. 1-5}$$

For the ionized water molecules[19], the produced primary radical species are hydroxyl radicals, hydrogen atoms, and electrons (in both pre-solvated states and solvated states) (Eq. 1-6).

$$H_2O^+ + H_2O \longrightarrow H_3O^+ + HO^\bullet \qquad \textit{Eq. 1-6}$$

$$H_2O^+ \longrightarrow HO^\bullet + H^+ \qquad \textit{Eq. 1-7}$$

$$e^- + nH_2O \longrightarrow e^-_{hyd} \qquad \textit{Eq. 1-8}$$

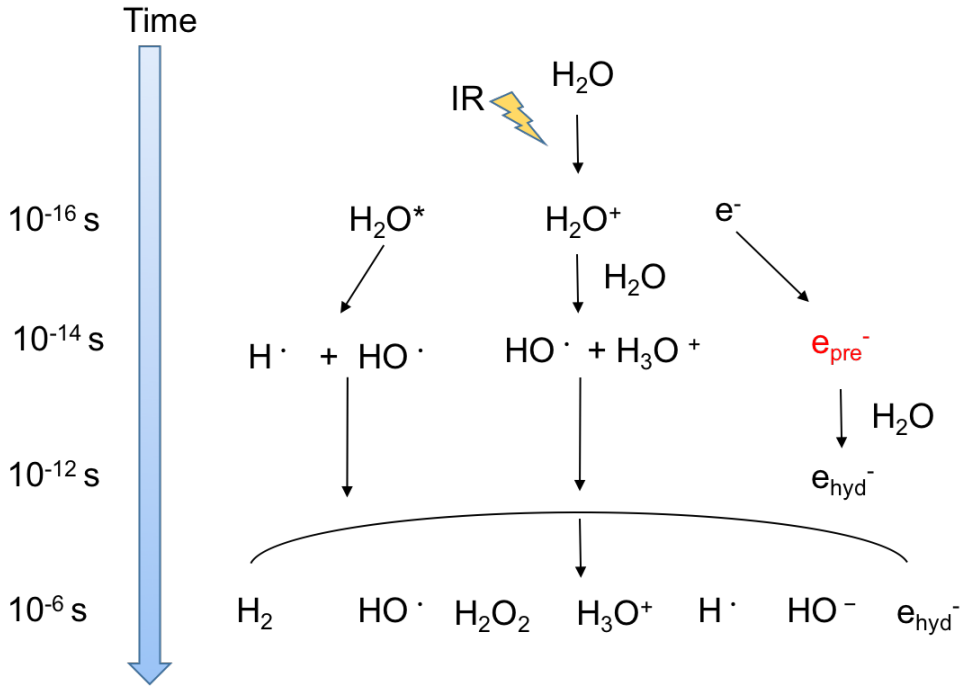

Figure 1-2. The time scale of events occurring in water radiolysis. Within 1 fs after irradiation, excited water molecules (H_20^*), ionized water molecules (H_20^+), and electrons (e^-) are produced. Then, femto-chemistry reactions, such as ion-molecules reactions (Eq. 1-6), dissociative relaxations (Eq. 1-7), and solvation of electrons (Eq. 1-8), occurs in 10^{-15}-10^{-12} s after irradiation. At ~10^{-6} s, radicals and reactive molecules diffuse in the solution and slow radical reactions produce indirect damages to a variety of cellular components. This figure is adapt from [20], [21].

In radiation chemistry, the yield of the altered entities is expressed by quantum yield, G value, which is a measurement of the number of formed (or destroyed) species per 100 eV energy absorbed by the entire sample:

$$G(X) = \text{number of species X formed} / \text{energy absorbed in 100 eV} \qquad \textit{Eq. 1-9}$$

For the radiolysis of water, the quantum yields of the dissociation products are reported to be 2.8, 2.4, 0.6 for the hydrated electrons (e_{hyd}^-), hydroxyl radicals ($OH^\bullet$), and hydrogen atoms ($H^\bullet$), respectively, at the microsecond time scale [18]–[22] (see Table 1-1). The quantum yields of these water radiolysis products are multifactorial. The G-value can be influenced by the temperature, the PH value of the system, as well as the type of radiation. The LET of the radiation beam will change the ratio of excited water molecules over ionized water molecules; therefore, alter the yields of different radio-lytic species. The quantum yields of the radical products ($OH^\bullet$, e_{pre}^-, and e_{hyd}^-) decrease while the LET of the radiation increases. High-LET particles can also enhance the efficiency of the recombination of the radical products to form molecular species (H_2O_2 and H_2)[23].

It is commonly agreed that the hydrated electrons are trapped in a reduction potential well of about -3.5 eV and they have a significant long lifetime in pure water comparing with other radicals; therefore, they are inactive in producing biological damages. The hydroxyl radicals are used to be thought as the most important radical that can induce oxidative damage during IR. However, based on the femtosecond laser spectroscopy discovery, it was confirmed that the pre-solvated electrons were the principle culprits to be blamed for the IR induced biologically damages.

Water radiolysis products	$OH^{\bullet}$	e_{pre}^{-}	e_{hyd}^{-}	$H^{\bullet}$	H_2O_2	H_2
G-Value (#/100eV)	2.4	7.5	2.8	0.6	0.8	0.4

Table 1-1. The quantum yields of the primary products from the radiolysis of liquid water. The fundamental role of e_{pre}^{-} played in radiation chemistry and biology was newly reported by our group based on our femtosecond time-resolved laser spectroscopy (fs-TRLS) measurement result[16], [24]–[26]. These quantum yields depend on many parameters, such as PH, temperature, and the LET of the radiation. Different types of radiation will alter the ratio of excited H_2O molecules over ionized H_2O molecules, subsequently alter the quantum yield of each formed species. The G-value of e_{pre}^{-} was estimated by considering 64% of the e_{pre}^{-} eventually becomes the long-lived e_{hyd}^{-}[21].

1.4 Pre-solvated electron

The hydration dynamics of electrons in pure water has long been a mystery since the 1960s[27]–[29]. With the pioneering work that was done by Ahmed H. Zewail and his co-workers[30], [31], the development of the ultrafast time-resolved laser spectroscopy technique has paved the way for scientists to obtain a much deeper understanding of the fundamental mechanisms of electron hydration. It was found that prior to the electrons eventually solvated in liquid water, there exist finite-lifetime (< 1 picosecond) precursor states called pre-solvated electrons (e_{pre}^-). In the year of 1987, the femtosecond time-scale lifetime of these pre-solvated electrons was first reported by Migus et al.[32]. After that, extensive follow up experiments have been conducted, but distinct physical proprieties and diverse ranges of lifetimes of e_{pre}^- were reported. By carefully applying effective e_{pre}^- scavengers, our lab demonstrated that there is a coherence spike in the current methodology of femtosecond time-resolved laser spectroscopy (fs-TRLS) measurement of e_{pre}^-. This coherence spike affects the accuracy of the pre-solvated electrons' lifetimes' measurement, and the uncertainty that the spike brings to the pre-solvated electron's lifetime spanning over two orders of magnitude[26]. Our lab has found that the intensity of the coherence spike has a linear dependence to the pump power. By utilizing this property, one can subtract the coherence spike from the transient absorption measurement. After the removal of the coherence spike, the life time of e_{pre}^- was determined precisely to be 540 ± 30 fs (as illustrated in Figure 1-3).

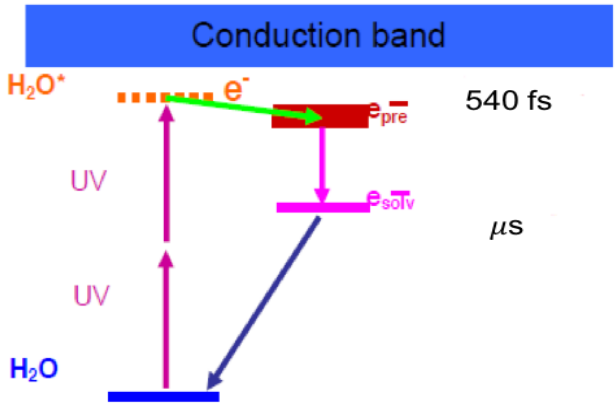

Figure 1-3. The schematic diagram illustrating the hydration dynamics of an electron in pure water. The per-solvated electron (e_{pre}^-) is generated via two-photon excitation of water molecules, and then, within 540 fs, the e_{pre}^- solvates to the equilibrium state to form the so-called hydrated electron (e_{hyd}^-). The e_{hyd}^- has a microsecond time-scale lifetime. Adapt from [26].

The solvated electron is surrounded by water molecules. Theses polarized water molecules can form a deep reduction potential well. The solvated electron is trapped inside of it and is less active in producing biological damages. While, the pre-solvated electron is a precursor state of the solvated electron, it is surrounded by less water molecules than solvated electron and therefore, it is weakly bonded. The weakly bond pre-solvated electron, unlike its solvated state, is more efficient in producing DNA damages. It has been a long controversy that at the molecular level, which water radiolysis species produces the most of biological damages. Conventionally, it is thought that e_{hyd}^- is less active in producing DNA damages and the majority of DNA damages are produced by $OH^\bullet$ radical. However, the conventional picture was drawn in the absence of e_{pre}^-. Due to its intrinsic high activity and high quantum yield, the fundamental role of e_{pre}^- played in radiation chemistry and biology must be taken into consideration. In order to investigate the DNA damages induced by each radiolysis species, our group has conducted an experiment by adding different scavengers (KNO_3, DMSO, and

isopropanol) to liquid DNA samples during IR[25]. KNO_3 is a scavenger for both e_{pre}^- and e_{hyd}^- ($OH^\bullet$ radical is one of the products from the KNO_3 scavenging reaction). DMSO and isopropanol are effective scavengers for both e_{pre}^- and $OH^\bullet$ radical. These results have shown that e_{pre}^- has a doubled efficiency in creating DNA strand breaks than the $OH^\bullet$ radical.

Based on the novel understanding on the lifetime and physical properties of e_{pre}^-, a new molecular mechanism of reductive DNA damage was proposed by our group. As shown in Figure 1-4, we illustrated that in the process of water radiolysis, e_{pre}^- and $OH^\bullet$ radical are the two radicals with the highest quantum yields. The $OH^\bullet$ radical can lead to oxidative DNA damages; while, the e_{pre}^- having a lifetime of ~540 fs can attach to DNA to induce future DNA damages via dissociative electron transfer (DET) reactions (See Section 1.6). Our lab has confirmed that, in terms of the productivity of DNA single strand breaks (SSBs) and double strand breaks (DSBs), the reductive mechanism via e_{pre}^- is at least twice as efficient as the oxidative mechanism via $OH^\bullet$ radical.

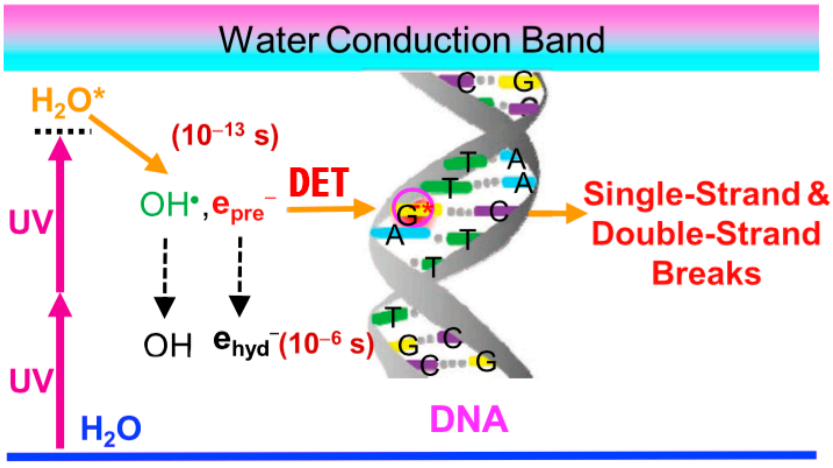

Figure 1-4. The schematic illustration of the reductive DNA damage mechanism. The e_{pre}^- and $OH^\bullet$ radical are the major water radiolysis products. It has been well-known that the $OH^\bullet$ radical can lead

to oxidative DNA damages, while it was newly confirmed that e_{pre}^- can cause reductive DNA damages (SSBs and DSBs) via the dissociative electron transfer (DET) reactions. This figure is adapted from [25]

1.5 Tumor hypoxia

During the process of aggressive malignant growth, the development of vascular network inside the solid tumors is severely limited and the vasculature inside a solid tumor is dramatically different from that of a normal tissue[33]. In the normal tissue, the blood supply is maintained by an evenly distributed vascular network. The hierarchically organized vascular network can efficiently furnish fresh oxygen and other nutrients via blood vessels while wash away metabolic wastes from the interstitium via the lymphatic system. However, inside of the solid tumors, due to the fact that pro-angiogenic and anti-angiogenic molecular factors are abnormally secreted, the vascular system is lack of hierarchy. The blood vessels are either immature, tortuous, or occluded[34], while the lymphatic vessels are either leaky, dilated, or discontinuous[35]. The irregular vessel structure results in impaired oxygen and nutrition flow. Acute and chronic micro-regional hypoxia are generated consequently. Hypoxia can induce apoptosis and necrosis in both normal and cancerous cells[36]. In the year of 1955, by investigating the histological section of tumor tissues surrounded by vascular stroma, Thomlinson et al. reported[37] that there should exist a decreasing gradient of oxygen partial pressure (pO_2) from the edge of the tumor cord toward its center; however, the cells between the necrotic center and the periphery of the tumor cord were still viable under hypoxic environment; therefore, they were more resistance to treatment.

Critical oxygen tension (mmHg)	Biological effects observed below critical oxygen tensions
0.2-15	Activation of hypoxia-inducible genes[38]–[41]
15-30	Resistance to photodynamic therapy[42]
25-30	Resistance to Low-LET radiation[43]–[45]
30-35	Resistance to interleukin-2 triggered immunotherapies[46]

Table 1-2. The inadequate oxygen supply inside solid tumors brings barriers to a variety of cancer treatments. Different hypoxia-induced biological effects were observed below different critical oxygen tensions. The oxygen partial pressure under which hypoxia-induced resistance to PDT, Low-LET radiation and immunotherapy can be observed were 15-30, 25-30, 30-35 mmHg, respectively. This table is adapted from [47]

Hypoxia can induce cell apoptosis and necrosis via different pathways. Hypoxia stimulates the expression of *p*53 gene, and *p*53 in a cell can be utilized as an indicator for the hypoxia induced *p*53-dependent apoptosis pathway, which involves Apaf-1 and caspase-9 as the downstream effectors[48]. The level of hypoxia-inducible factor-1 (HIF-1) can also be introduced as an indicator for the hypoxia-induced *p*53-independent apoptosis pathways[49]. Paradoxically, hypoxia-induced genome and protein changes can also promote the cancer cells to adapt to their hostile environment and, therefore, enhance the cancer cells' proliferation and bring barriers to cancer treatments. A great portion of the hypoxia-inducible genes are regulated by transcription factors, such as HIF-1 and nuclear factor κB (NFκB). The threshold of oxygen partial pressure required to activate these hypoxia-induced transcription factors were reported to be under 15 mmHg for a variety of cancer cell lines

(see Table 1-2). Even though lack of quantitative data of hypoxia-induced chemo-resistance, a few in vitro and in vivo experiments have qualitatively shown that the potency of some chemotherapy agents, such as carboplatin and cyclophosphamide, were also oxygen dependent[50]–[52]. For immunotherapy, it was reported that the effectiveness of the interleukin-2 stimulated T-cell killing of cancer cells started to decrease when oxygen level was less than 35 mmHg (see Table 1-2).

The hypoxic microenvironment inside of the solid tumors has also been a severe problem in cancer treatment, both photodynamic therapy and radiation therapy[45]. The potency of photodynamic agents and Low-LET radiation (x-ray radiation and γ-ray radiation) will be limited when the oxygen partial pressure is under 15-35 and 25-30 mmHg, respectively (See Table 1-2). The oxygen enhancement ratio (OER) is a measure of the enhancement of therapeutic effect under the exposure of IR in the presence of oxygen compared to the absence of oxygen. As shown in Eq. 1-10, the OER is defined as the ratio of the radiation dose required in hypoxia over the radiation dose required in normoxia to achieve the same level of biological effect.

$$\text{OER} = \text{radiation dose in hypoxia} \Big/ \text{radiation dose in normoxia} \qquad \textit{Eq. 1-10}$$

As the response of a cell to ionizing radiation strongly depends on its oxygen concentration, in the presence of oxygen, the radiation dose required to achieve the same tumor control probability is generally only one third of the dose required in the absence of oxygen (OER ≈ 3)[43], [44], [53]. Therefore, oxygen is a potent radiosensitizer and its radiation enhancement mechanisms were thought to rise from two aspects: 1) the oxygen fixation hypothesis (OFH)

(see Eq. 1-11)[54] and 2) the formation of oxygen free radicals, dominantly the superoxide radicals ($O_2^{\bullet-}$) (see Eq. 1-12)[55].

$$\begin{gathered} DNA + e_{pre}^{-} / {}^{\bullet}OH \rightarrow {}^{\bullet}R \text{ (DNA Damage)} \\ {}^{\bullet}R + O_2 \rightarrow {}^{\bullet}RO_2 \text{(Damage fixed)} \end{gathered} \qquad \textit{Eq. 1-11}$$

$$e_{pre}^{-} + O_2 \rightarrow O_2^{\bullet-} \rightarrow \text{DNA Damage} \qquad \textit{Eq. 1-12}$$

The OFH was first developed in the 1950s and was widely accepted as the radiochemistry rationale for oxygen sensitizing effects[56]. Based on our unique understanding of the prosperities of per-solvated electrons, this hypothesis can be explained by the following processes (see Eq. 1-11): During IR, pre-solvated electrons and hydroxyl radicals are the major radical products with the highest quantum yields from water radiolysis; DNA is the principle target for these radicals and intensive indirect DNA damages will be produced by these radicals. In the absence of molecular oxygen, these DNA damages could be chemically repaired to their original state efficiently; while, in the presence of oxygen, the oxygen molecule will attach to a DNA damage site to form a non-restorable preoxy radical ($^{\bullet}RO_2$), and make DNA damages hard to be repaired by the cell itself. In the latter case, the radical damages are thought to be ‘fixed’.

If the mechanism of the oxygen effect in radiation therapy is solely a chemical process, as the OFH postulated, the production of the non-restorable preoxy radical should not depend on genetic identity of the irradiated cells. In the year of 1998, by exposing three different wild-

type strains of *E.coli* to radiation, Ewing David showed that the maximum dose that did not alter the *E.coli* cells' survival fraction was strain dependent. This experiment suggested that the OFH may not complete. Special attention must be given to the fact that even though, the fundamental chemistry proposed in the OFH is correct, OFH may not be able to cover the biological and enzymatic DNA repair pathways.

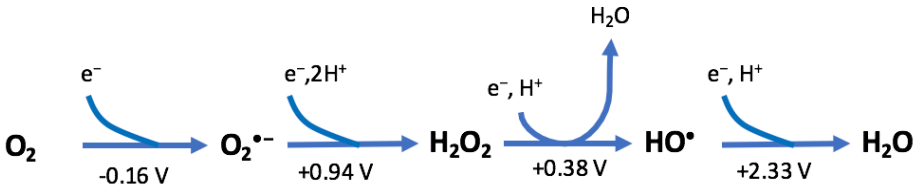

Figure 1-5. The schematic illustration of the four-step single-electron reduction mechanism converting a molecular oxygen to a water molecule. The standard reductive potentials for each dioxygen derived product were listed respectively. These values were obtained from aqueous solution with oxygen at the standard atmosphere, PH value =7. This figure is adapted from [57].

In the other aspect, the reduced production of superoxide radicals in the hypoxic environment could be another explanation of why a well-oxygenated cell requires less radiation dose to achieve the same level of cell killing effect comparing to a hypoxia cell.

Radicals and molecules derived from molecular oxygen is the most important class of species that generated in a living system. They have substantial impact on many essential biological processes[58], [59] and are so-called reactive oxygen species (ROS). The four steps of the one-electron reduction mechanism that covers a molecular oxygen to a water molecule are illustrated in Figure 1-5. The formation of superoxide radical ($O_2^{\bullet-}$), hydrogen peroxide,

hydroxyl radical and water molecule are stepwise shown with their standard reduction potential. As a consequence of the fact that superoxide radical is the first step product of the the entire reduction mechanism, the productivity of superoxide radical is the highest among all these species. It is reported that more than 2% of the total oxygen consumed in aerobic metabolism is utilized to produce superoxide radicals and the average annual production of superoxide radical in human is about 2 kg[60]–[62]. The superoxide radical has a slightly negative reductive potential (-0.16 V) and due to its unpaired electron, the superoxide radical has a considerable degree of activity. Conventionally, it was thought that superoxide radical can act both as a reducing agent[61] (Fe^{3+} can be reduced to Fe^{2+} by $O_2^{\bullet -}$) and as an oxidizing agent[63] ($O_2^{\bullet -}$ can oxidize the thiol groups). Our group has recently revealed the function of $O_2^{\bullet -}$ in producing severe reductive DNA damages and suggested that $O_2^{\bullet -}$ might act as a strong reducing agent in many pathological and physiological processes[64].

Under normal circumstances, the majority of superoxide radicals are generated within mitochondria in a biological system. Mitochondria synthesize adenosine triphosphate (ATP), the fuel that drives all of the physiological activities, through a mechanism that is so-called the electron transport chain (ETC)[65]. Even under an ideal condition, some electrons can still leak from ETC and interact with oxygen to form superoxide radicals. Except for mitochondria, other cell organelles such as endoplasmic reticuli, lysosomes and cytoplasmic membranes can also generate superoxide radicals during their routine hydroxylation and oxidation reactions[57]. It is noteworthy that superoxide radicals are more likely to be generated in the cell organelles rather than in the nucleus; therefore, the organelle genes have higher tendencies to be damaged by superoxide radicals under usual circumstances.

Under unusual circumstances where exogenous stresses such as ionizing radiation or ultraviolet photons are presented, the formation of superoxide radicals can be mediated non-enzymatically[66]. Pre-solvated electrons can be generated inside the nucleus from the radiolysis of water. When oxygen molecule is close to the pre-solvated electron, the electron will attach to the oxygen molecule to form a superoxide radical. The superoxide radicals can be eliminated by a cell either spontaneously or by superoxide dismutase (SOD) and the energy of the superoxide radicals are also transferred to nucleus DNA (see Eq. 1-12) and other subcellular targets along these processes. In the aqueous environment inside a cell, the superoxide radical has a very short lifetime[67], [68] and cannot diffuse far enough to produce significant direct damages. However, it has an electron affinity about -0.5 eV. The negative electron affinity suggested that superoxide radical has the tendency to donate one electron rather than capture one. Therefore, it is relatively easy for a superoxide radical to eject an electron and be oxidized. When the ejected electron is attached to DNA, the dissociative electron transfer reaction will inflict DNA to cause bound rupture, nucleotide breakage, and other irreversible *reductive* DNA damages[64].

For hypoxia cancer cells, the limited intrinsic oxygen level accounts for the fact that excess of pre-solvated electrons exist after exposing to IR (the pre-solvated electrons are less likely to be eliminated through Eq. 1-12). There is no doubt that pre-solvated electrons can create severe DNA damages; however, considering pre-solvated electrons' ultrashort lifetimes, high reactivity, and the complex environment inside a tumor cell, a compound that can mimic the mechanism of oxygen by letting a pre-solvated electron weakly bond to it and producing

further DNA damages via DET reaction would be a good candidate to increase the IR induced indirect DNA damages in hypoxic cells.

1.6 DET based radiosensitizer

The definition of "dissociative electron transfer (DET)" is an ultrafast electron transfer (~femtosecond) of a weakly bound electron to a transition molecule, AB, and then the chemical bond of AB is broken, AB dissociates into fragments:

$$e^{-}(<0\ \text{eV}, <1\text{ps}) + AB \rightarrow AB^{*-} \rightarrow A\ (+ B^{-}) \rightarrow \text{DNA damage} \qquad \textit{Eq. 1-13}$$

As the definition suggested, the term "DET" refers to a process occurs when a weakly-bound electron (< 0 eV) from either an atom, a molecule, or the polar medium rapidly transfers to a transition molecule, forming a transient negative ion (TNI). Then, the fragments (A and B) will be produced from the dissociation of the TNI. As shown in Eq. 1-13, when considering DNA is the target, the dissociated AB fragments could be radicals and the resultant radicals could inflict DNA damages. The source of the electron could either the radiolysis of bio-molecules (most likely the water molecules) under ionizing radiation or the reductive intracellular environment of a cancer cell.

Based on our fresh understanding about the properties of pre-solvated electrons, a family of compounds with radiosensitivity through the DET reaction have been discovered by our group by utilizing the fs-TRLS techniques[16]. These compounds are so-called femotomedicine (FMD) compounds. In-vivo and *in vitro* experiments have already shown that these FMD compounds are potent anticancer agents for chemotherapy and could be effective radiosensitizer for radiation therapy[16], [69]. The advantages of these FMD compounds over the conventional platinum-based anticancer agents are 1) the FMD

compounds do not contain platinum (the heavy metal which is cytotoxic and hard to be eliminated by human body); therefore have better pharmacokinetic properties; 2) the FMD compounds have the natural selectivity that shown far less cytotoxicity and radiotoxicity on human normal cell lines than on the human tumor cell lines[16], [69]; 3) the FMD compound molecules are sufficiently effective in DET reactions and the DET reactions could be even more effective in hypoxia tumor environment.

The DET reaction of the FMD compound can be described as the following: Pre-solvated electrons are either created from IR of water or from the reductive environment of a cancer cell. If pre-solvated electrons are not captured by a transition molecule (either a FMD compound or DNA), they will quickly get solvated by the surrounding water molecules to form solvated electrons. When a FMD compound is present, the pre-solvated electron will dissociatively attached to a FMD compound and the negative transient ion, FMD^{-}, will be formed. The potential energy curve for FMD^{-} is much lower than the potential energy curve for the FMD; therefore, the ultrafast effective resonant DET will occur and FMD compound will dissociative into fragments. These resultant radical fragments can effectively cause DNA damages and subsequently kill the cancer cells.

In the presence of molecular oxygen, there should be a competition binding of pre-solvated electrons between FMD compound molecules and oxygen molecules. Due to the fact that FMD^{-} compound molecules are more efficient in producing DNA damages than the $O_2^{\bullet -}$, the FMD compound should be more effective in the hypoxic environment than in the normoxic environment. The major task in this project is to carry out *in vitro* tests to verify if the FMD

compound's radiosensitizing effect is enhanced in hypoxia cancer cells and to perform quantitatively analysis, to calculate the enhancement ratio.

Chapter 2 Steady-state absorption spectra analysis of the radiolysis of the FMD compound

2.1 Introduction

Spectroscopy is one of the most fundamental techniques in analytical chemistry study and biochemical study. It is a quantitative measurement of the interaction between electromagnetic (EM) radiations and the irradiated samples. In the 17th century, by refracting white sunlight beams with a prism, Isaac Newton provided the first scientific analysis of spectroscopy in the world. There are many types of spectroscopy that have been developed, such as atomic absorption spectroscopy, Raman spectroscopy, microwave spectroscopy, fluorescence spectroscopy, ultraviolent/visible (UV/Vis) spectroscopy, infrared (IR) spectroscopy, nuclear magnetic resonance (NMR) spectroscopy, etc. Among all these techniques, the UV/Vis spectroscopy provides researchers the simplest and cheapest way to get an access to a variety of properties of a sample, such as the concentration of a sample, the solubility of a solute, the rate constant of a reaction, etc. Therefore, the static UV/Vis spectra measurement was chosen as the first experiment in this thesis.

The simplified working mechanism of a single beam UV/Vis spectroscopy is illustrated in Figure 2-1. A UV/Vis spectroscopy consists of three parts, they are 1) a lamp, 2) a monochromator, 3) a cuvette holder and 4) a photodetector. The lamp provides a continuous

stable light source from ultraviolet region to visible region for the system. The monochromator separates the light beam into different fractions spatially by the wavelength. The light beam with the selected wavelength can pass through the cuvette holder and the intensity of the transmission light is recorded by a photodetector. The data is collected by the data acquisition card and the spectrum is then plotted for future analysis. For solutions at low concentration, the absorbance of the incident light by the sample can be described by the Lambert-Beer's Law.

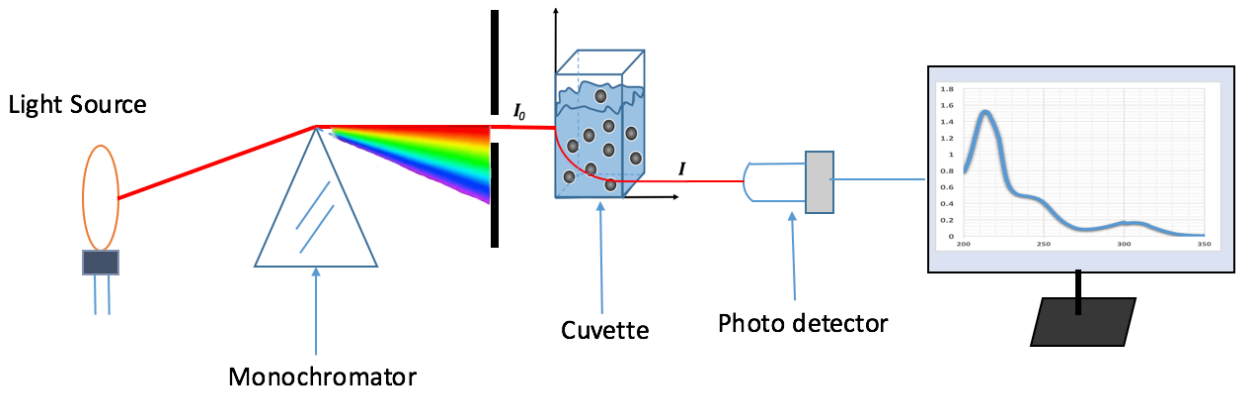

Figure 2-1 A simplified schematic illustration of the working function of a UV/Vis spectroscopy. Light beam with a specific wavelength is generated from a monochromator. After passing through a cuvette which contains the sample, the light intensity is decreased and the signal is recorded by a photodetector. The absorbance of incident light is described by the Lambert-Beer's Law.

As shown in Figure 2-2, the Lambert-Beer's law is a famous quantitative relationship between the concentration of a coloured substance in a homogeneous solution and the amount of light the solution absorbed.

$$Abs = \log\left(I_0 / I\right) = \varepsilon lc \qquad \text{Eq. 2-1}$$

Where Abs is the absorbance of the sample, I_0 is the intensity of the incident light, I represents the intensity of the transmission light, ε is the molar extinction coefficient, l is the length that the incident light travels, and c is the molar concentration of the solute.

The geometric properties of a given cuvette are fixed, which means the distance that the incident light travels, l, is a constant. At low concentrations, the molar extinction coefficient is a constant, the molar extinction coefficient, ε, is a constant; therefore, a linear relationship between absorbance of the sample and the concentration of the substance is expected.

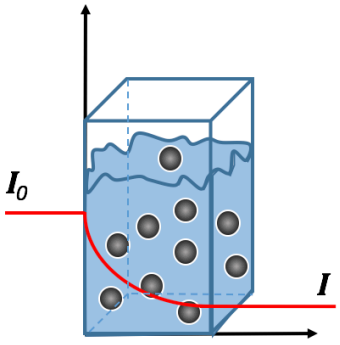

Figure 2-2. The schematic illustration of the Lambert-Beer's Law. The incident light is absorbed by the solute, and the intensity of the transmission light is therefore attenuated along the path. Based on the Lambert-Beer's Law, the absorbance is proportional to the concentration of the solute.

2.2 Method

2.2.1 Chemicals and reagents

To prepare the FMD compound stock solution, 5.3 mg of the FMD compound was weighted by an analytical balance and then dissolved in 1000 μL of ethanol to make a 20 mM FMD compound stock solution. For this steady-state absorption spectroscopy experiment, the 100 μM FMD solution sample was prepared by mixing 150 μL of the 20 mM FMD compound stock solution with 30 mL of ultrapure water (TOC< 1ppb, Resistivity = 18.2 MΩ-cm). The ultrapure water was directly obtained from the Barnstead Nanopure water system.

2.2.2 Steady-state absorption spectroscopy

All the steady-state absorption spectra in this chapter were obtained using a Beckman Coulter DU 530 UV/Vis spectroscopy. First, 400 μL of the FMD solution sample (100 μM) was added into a cuvette, the steady-state absorption spectrum was then measured. The peak of the absorption spectrum was in the range of 1.5-1.7, which proved that the Lambert-Beer's Law can be applied to this sample. Then, different quartz cuvettes were filled with 400 μL of the sample and are either bubbled with air, nitrogen, or argon gas for half an hour, protected from light. After bubbling, totally 40Gy of radiation dose was evenly divided into 4 fractions (10Gy each) and applied to the cuvettes. The steady-state absorption spectra of these cuvettes were then measured before and after irradiation.

2.2.3 Hypoxic environment system

To create a hypoxic environment, the cuvettes that contained the FMD solution samples were bubbled with compressed nitrogen and argon gas. The high purity nitrogen and argon gas were ordered from Praxair, and the purity was > 99.998%. For the control group, the samples were bubbled with air. The bubbling system, as shown in Figure 2-3, was consisted with a long needle, a short needle, and a rubber plug with parafilm wrapped around it. The gas was bubbled into the cuvette through the long needle and was exhausted through the short needle. The cuvette was sealed with a rubber plug and parafilm. The sample was prevented from light, and was bubbled for half an hour with a constant rate (1-2 bubbles per second).

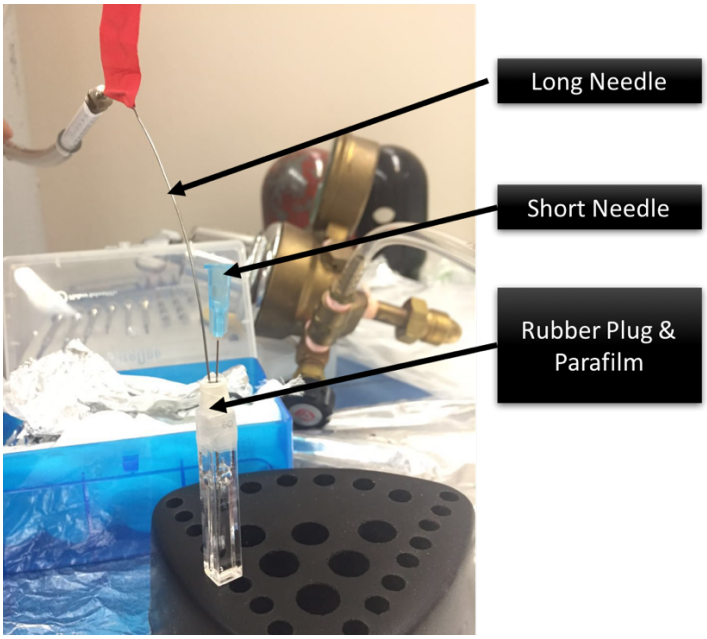

Figure 2-3. The experimental apparatus diagram of the bubbling system. The gas flows into the cuvette through the long needle, which was immersed into the very bottom of the cuvette. The short needle, which was above the fluid level, acted as the exhaust vent. The system was sealed by the rubber plug and parafilm.

2.3 Results

To determine if the FMD compound is sensitive to IR, 400 µL FMD solution sample (100 µM) was added into a cuvette, bubbled with air for half an hour, and then irradiated with 10Gy X-ray radiation 4 times. The steady-state UV/Vis absorption spectra of the sample were measured before and after irradiation. The difference spectra between each irradiated sample and the control group (without exposing to IR) were also plotted (see Figure 2-4). The difference spectra were amplified by 10 times. Each of the difference spectra has a peak at 220 nm. The decrease of the absorbance after irradiation shows that FMD compound is indeed sensitive to X-ray radiation.

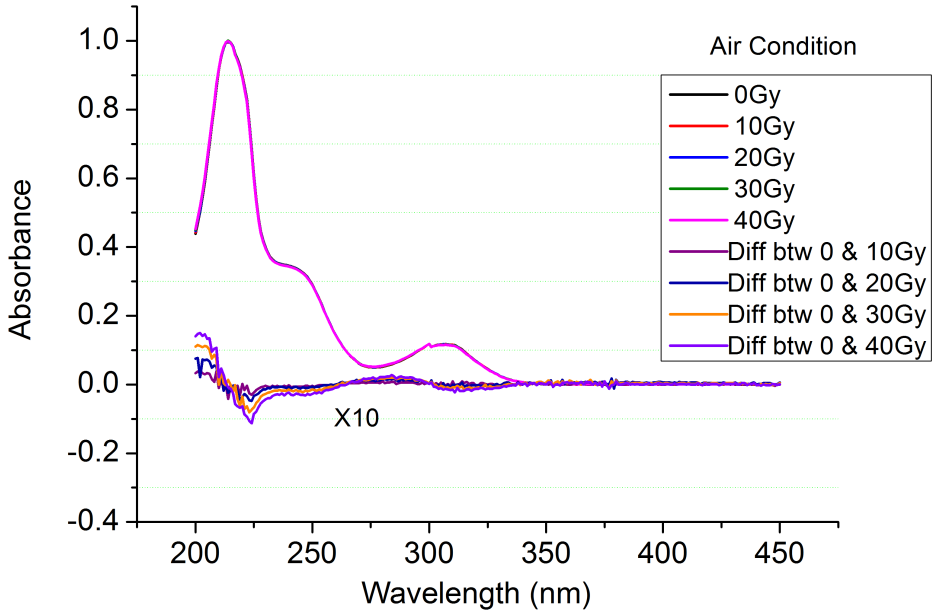

Figure 2-4. The steady-state UV/Vis absorption spectra of the FMD solution sample (100 µM) after being exposed to different doses of IR. These spectra were measured at room temperature. Prior to radiation, the sample was bubbled with air for half an hour, protected from light. The difference

spectra between each irradiated samples and the control group were also plotted. The decrease of absorbance suggested that FMD compound is sensitive to IR.

To determine if the FMD compound is more sensitive to IR in the hypoxic environment, 400 μL FMD solution sample was added into a cuvette, then the FMD solution sample was bubbled with nitrogen, instead of air, for half an hour, protected from light. 40 Gy of X-ray was applied to the sample in 4 fractions. The UV/Vis absorption spectra were measured before and after being exposed to IR. The results were shown in Figure 2-5. In order to exclude the effect of the reactive nitrogen species, this experiment was repeated by bubbling the sample with argon gas. The results were also shown in Figure 2-5. The difference spectra were plotted. It seems that the difference spectra of samples bubbled with nitrogen were identical with the difference spectra of samples bubbled with argon. By comparing the difference spectra of the N_2/Ar bubbled sample with the difference spectra of the air bubbled sample, one can see that in hypoxic environment, the FMD compound is more efficiently dissociated by IR. As all the difference spectra have a peak at 220 nm, the absorbance decrease of the samples at 220 nm has provided us a quantitative measurement of radiosensitivities of the FMD compound in either air, N_2, or argon conditions. The decrease rate of FMD compound was calculated as the change of absorption over the change of radiation dose, and it can be obtained from the linear fit of the radiation induced absorbance decrease at 220nm. As shown in Figure 2-6 , in nitrogen and argon condition, the decrease rates were almost the same (0.0170 ± 0.0008), in air condition, the decrease rate was 0.0015 ± 0.0005. The hypoxic environment enhanced the radiosensitivity of FMD compound by about 9 times.

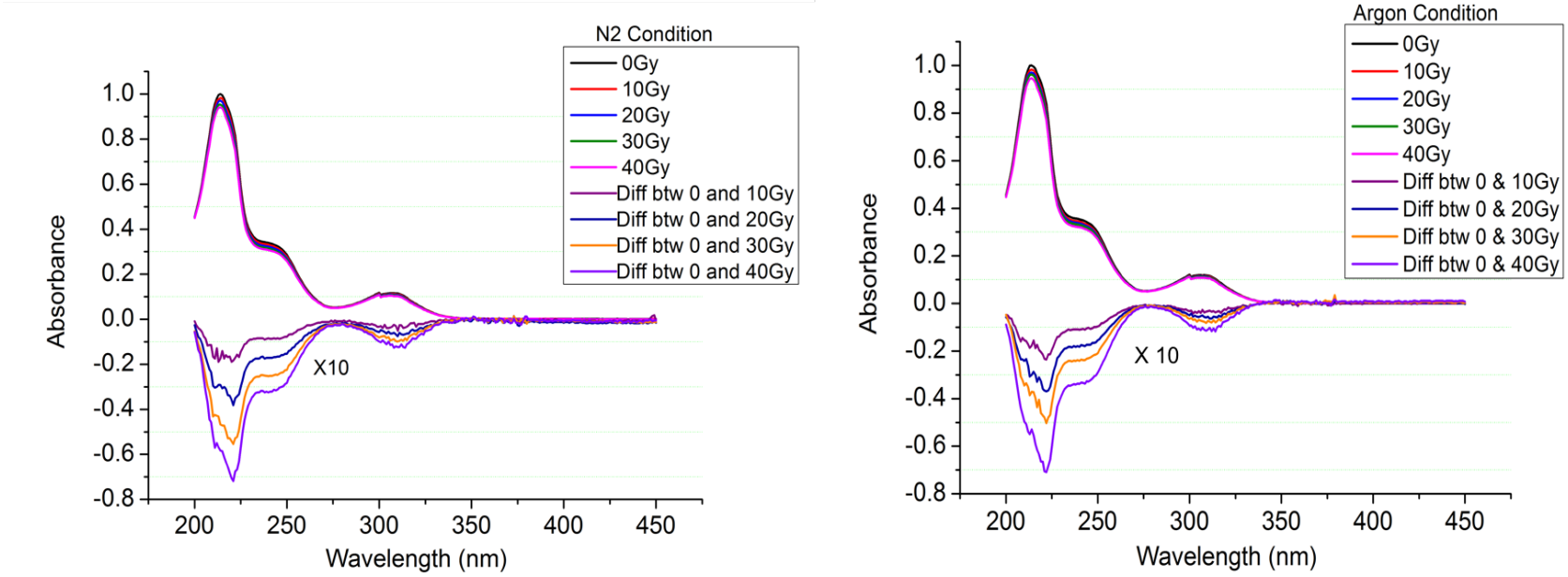

Figure 2-5. The steady-state UV/Vis absorption spectra of the FMD solution sample (100 μM) exposed to different dose of IR. The spectra were measured at room temperature. Prior to radiation, the sample was bubbled with N_2/Argon for half an hour, protected from light. The difference spectra between each irradiated sample and the control group were also plotted. The difference spectra were magnified by 10 times.

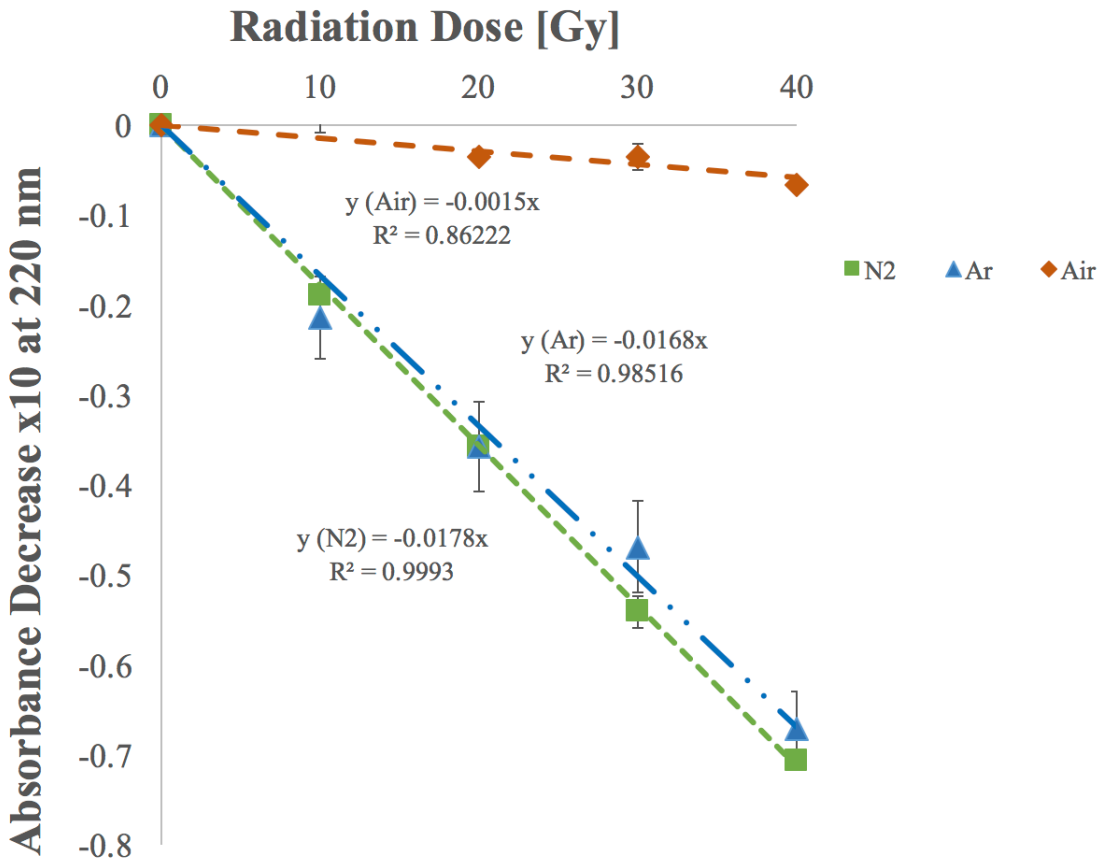

Figure 2-6. The absorbance decrease at 220 nm of the irradiated FMD solution sample (100 μM). The samples were irradiated by different doses of X-ray under either air, nitrogen, or argon gas environment. The decrease rate showed a linear dependent to the radiation dose. The decrease rates were obtained from the linear fit of the radiation induced absorbance decrease. In nitrogen and argon environment, the decrease rates were almost the same (0.0170±0.0008), which was 9 times faster than the decrease rate in air environment (0.0015±0.0005).

2.4 Conclusion

In this experiment, we confirmed that the FMD compound is sensitive to IR. This is one of the most fundamental characteristics for a potential radiosensitizer. By comparing the decrease rates of the steady-state absorption spectra of the irradiated FDM compound solutions, we also confirmed that under hypoxic environment, the radiosensitivity of the FMD compound was increased by 9 folds. The mechanism is proposed to be as the following:

- In the presence of oxygen, after the radiolysis of water, e_{pre}^- will either be captured by oxygen molecules to form the $O_2^{\bullet -}$ radicals, or dissociatively attached to FMD molecules. If it is attached to the a FMD molecule, the FMD molecule will dissociate into fragments; therefore, the absorbance of FMD compound will be reduced. The dissociative FMD radical fragments might have anticancer activities (will be discussed in next chapter); therefore, after dissociation, the FMD compound is considered to be activated (see Eq. 2-1).

$$e_{pre}^- + O_2 + FMD \rightarrow O_2^{\bullet -} + FMD^{\bullet -} \rightarrow \text{Activated FMD} \qquad \textit{Eq. 2-2}$$

- In the absence of oxygen, there will be no competition binding of e_{pre}^- between molecular oxygens and the FMD compounds. Therefore, more FMD compounds will dissociate into radical fragments due to the excess of e_{pre}^- (see Eq. 2-2).

$$e_{pre}^- + FMD \rightarrow FMD^{\bullet -} \rightarrow \text{More Activated FMD} \qquad \textit{Eq. 2-3}$$

Chapter 3 *In vitro* DNA double strand breaks measurement

3.1 Introduction

Exogenous stress, such as cytotoxic chemical agents, ionizing radiation beams, or ultraviolent light, can lead to a variety of DNA damages in a tumor cell. Some of the DNA damages, such as base alterations and single strand breaks, can be instantly repaired by a cell. Among all these DNA damages, double strand break (DSB) is the most lethal type. During the normal life of a cell, the genome damages of the cell are continuously arising, but the DSBs are rare events. Cells, especially cancer cells, may lack of enzymes to correctly repair double strand breaks comparing to that for other types of DNA damages[71]. Therefore, double strand breaks are very difficult to be repaired, and if not repaired correctly, fusions, deletions, and translocations could happen in the adjacent DNA sequences, programmed cell death (apoptosis) will be initiated[72].

Currently, there are many methods that are used for the detection of DNA DSBs, such as gel electrophoresis, pulsed-field gel electrophoresis (PFGE)[73], and γ-H2AX labeling. The gel electrophoresis can be used to detect DNA fragments less than 50kb, the PFGE can be used to isolate DNA fragments with higher molecular weights. By utilizing γ-H2AX labeling, DNA DSBs can be visualized with cell-by-cell resolution, and can be quantified through fluorescence microscopy, without rupturing the cell membranes and extracting the DNA.

Therefore, γ-H2AX labeling has become an increasingly popular succedaneum to the other DNA DSBs detection methods.

In mammalian cells, DNA is wound on histone-groups to form a condensed structure unit, which is called a nucleosome. In the center of each nucleosome core particle, there is an octamer of core histones, which is warped by about 146 base pairs of DNA[74]. The histone octamer is consisting with one H3/H4 tetramer and two H2A/H2B dimmers. Therefore, H2A, as one of the core histones, has substantial impact on the formation of nucleosomes as well as the function of DNA. H2AX is a subtype histone belongs to the H2A histone family. H2AX can be phosphorylated in the position of Ser139 by kinases such as ATM (ataxia telangiectasia mutated), ATR (ATM-Rad3-Related), or DNA-PK (DNA dependent protein kinase)[75]. Within a few minutes after exposing to genotoxic agents or ionizing radiation, DNA DSBs will take place. In the adjacent to the breaks, H2AX will be phosphorylated[76]. The phosphorylated H2AX, γ-H2AX, is essential for the assembly of DNA repair proteins and for the activation of checkpoints proteins[77]. The γ-H2AX foci have a 1:1 relationship with DSBs[78]; therefore, γ-H2AX can be used as a biomarker to represent DNA DSBs. To visualize the DSB by immunofluorescence, we first add γ-H2AX antibodies to selectively detect the γ-H2AX foci, then secondary antibodies are added for the amplification of the fluorescence signal.

3.2 Method

3.2.1 Cell culture

The human lung cancer cells, A549 (ATCC® CCL-185™) were purchased from the American type culture collection (ATCC). Cells were grown in Kaighn's Modification of Ham's F-12 (F-12K) medium supplemented with 10% fetal bovine serum (Invitrogen) and 1% penicillin-streptomycin (PS) solution (ATCC® 30-2300™). The cells were incubated in 10% humidified atmosphere with continuous 5% of CO_2 supply at 37 ℃, and were passaged twice a week.

3.2.2 Radiation treatment

The logarithmic phase A549 cells were seeded in black 96-well plates at a density of 2500 cells/well. Following a 24 hours' incubation, in order to let the cells attached to the bottom of the plates, the cell culture medium in the plates was replaced by fresh medium containing either 0 or 40 μM of FMD compound. Cells were incubated for 6 hours. After that, the plates for the hypoxia treated cells were placed in our hypoxic environment system for 2 hours; while, the plates for the normoxic cells remain in the incubator. Then, the plates were irradiated with either 0 or 10 Gy of X-Ray dose by a 225 KV X-ray machine (Precision, X-RAD IR225) at a dose rate of 2.5 Gy/mins. After IR, the hypoxia treated cells were taken from our hypoxic environment system and incubated together with the normoxic cells for two days. After the two days' incubation, the γ-H2AX detection assay was performed to the cells. The yield of DSBs were analysed by the software Image J (See Figure 3-1).

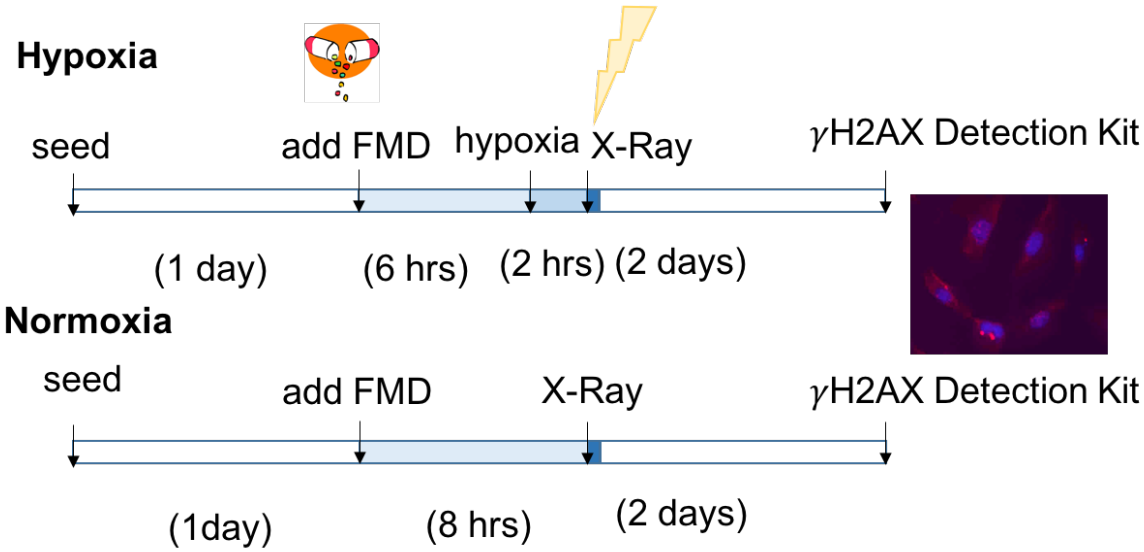

Figure 3-1. The schematic diagram of the radiation treatment of A549 cells. Following a 24 hours' incubation, the cells were treated with 0 /40 μM of FMD compound for 8 hours. For hypoxia treated cells, in the last two hours of the 8 hours' drug treatment, plates were sealed in our hypoxic environment system. Then 10 Gy of X-ray was applied to the cells. After radiation, the cells were incubated for 2 days in a regular cell incubator. Eventually, γ-H2AX detection assay was performed to the cells.

3.2.3 Hypoxic environment system

The hypoxic environment system (see Figure 3-2) was designed with the help of my colleague, Wei Hong, and the idea was inspired by Wang et al. [79]. In brief, the hypoxia condition was achieved by flowing compressed gas mixture (95% N_2, 5% CO_2, directly ordered from Praxair) into a large Ziploc® double zipper produce bag (purchased from Walmart). The working process is described as the following: a multi-well plate was placed into the zipper bag in advance, then the bag was flushed by the gas mixture for 3 times before the bag was filled with the gas and sealed. The sealed bag was then placed in an incubator for 2 hours at 37 ℃. Once sealed, it took 0.5-2 hours for the oxygen concentration eventually

reached equilibrium between the cell culture medium (inside the multi-well plate) and the surrounding gas mixture[79], [80]. Therefore, during the 2 hours' hypoxia treatment, the gas inside the zipper bag was refilled 6 times in order to extirpate any oxygen, which may emit from the cell culture medium.

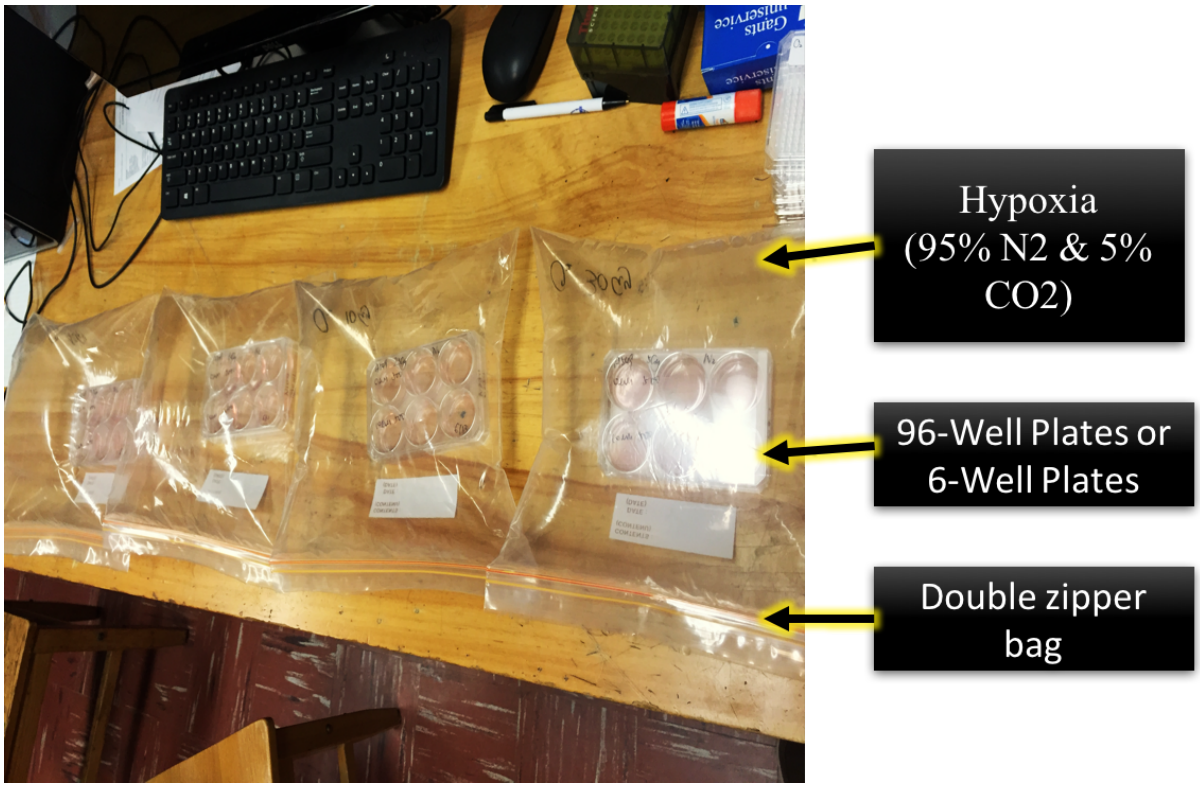

Figure 3-2. The experimental apparatus diagram of the hypoxic environment system. The cancer cells were seeded in the multi-well plates, and the plates were sealed in double zipper bags which contains 95% N_2 and 5% CO_2. The sealed bags were incubated at 37 ℃ for a desired period of time, then X-ray was applied to the cells which were sealed in the double zipper bag.

3.2.4 γ-H2AX detection kit

HCS DNA damage kit (Invitrogen, Catalog # H10292) was used in this experiment for the detection of the DNA DSBs. In this kit, Alexa Fluor® 555 goat anti-mouse IgG was used to selectively bind to the DNA DSBs sites and produce red emissions. The Hoechst 33342 was used to stains nuclear DNA and produce blue emissions. This kit was used following the standard protocol provided by the manufacturer. In brief, Image-iT DEAD Green™ viability stain was added to the cells and the cells were incubated for half an hour in a regular cell incubator. Then, the cells were fixed, permeabilized, and blocked. Following that, the γ-H2AX primary antibody, Alexa Fluor® 555 secondary antibody, and Hoechst 33342 nuclear counterstain were added to cell sequentially. Finally, the cells were washed thoroughly to remove all the excess antibodies. The immunofluorescence microscopy pictures of the cells were taken by a Nikon Eclipse TS1000 microscope, and the intensity of γ-H2AX per cell was quantitatively analysed by Image J software.

3.3 Results

To determine if the FMD compound can induce more DNA DSBs in hypoxic environment, A549 cells were treated with/without 40 μM of FMD compound and exposed to 0/10Gy of X-Ray radiation in normoxia/hypoxia conditions. The yield of DNA DSBs were represented by the intensity of γ-H2AX per cell. The images were shown in Figure 3-4. The blue fluorescence represents the stained nuclear DNA and the red fluorescence is from the γ-H2AX foci. A quantitative analysis of the yield of γ-H2AX was shown in Figure 3-3.

First, by comparing the yield of DNA DSBs (intensity of the γ-H2AX foci) between the control groups (the groups without FMD compound treatments), one can see that the 2 hours' hypoxia treatment increased the yield of DSBs for the non-irradiated cells, but decreased the yield of DSBs for the irradiated cells. The increase could be explained as the hypoxic environment introduced exogenous stress to the cancer cells, and it therefore increased the instability of the DNA; while the decrease can be explained by the oxygen enhancement effect as discussed thoroughly in the previous chapter. In the absence of oxygen, the DNA DSBs will not be fixed by oxygen and there is also no $O_2^{\bullet -}$ to damage to DNA through the DET reaction, the yield of DSBs in the hypoxic environment are therefore less than the yield of DSBs in the normoxic environment. The decrease also proved that our hypoxic environment system successfully maintained the low level of oxygen during the experiment period.

Then, by comparing the groups that were treated with 40 μM of the FMD compound, one can see that even though the FMD compound showed some genotoxicity for the non-irradiated cells, an increase of DNA DSBs was observed both in normoxic environment and in hypoxic environment after radiation. Moreover, the increase in the hypoxic environment is more significant than that in the normoxic environment.

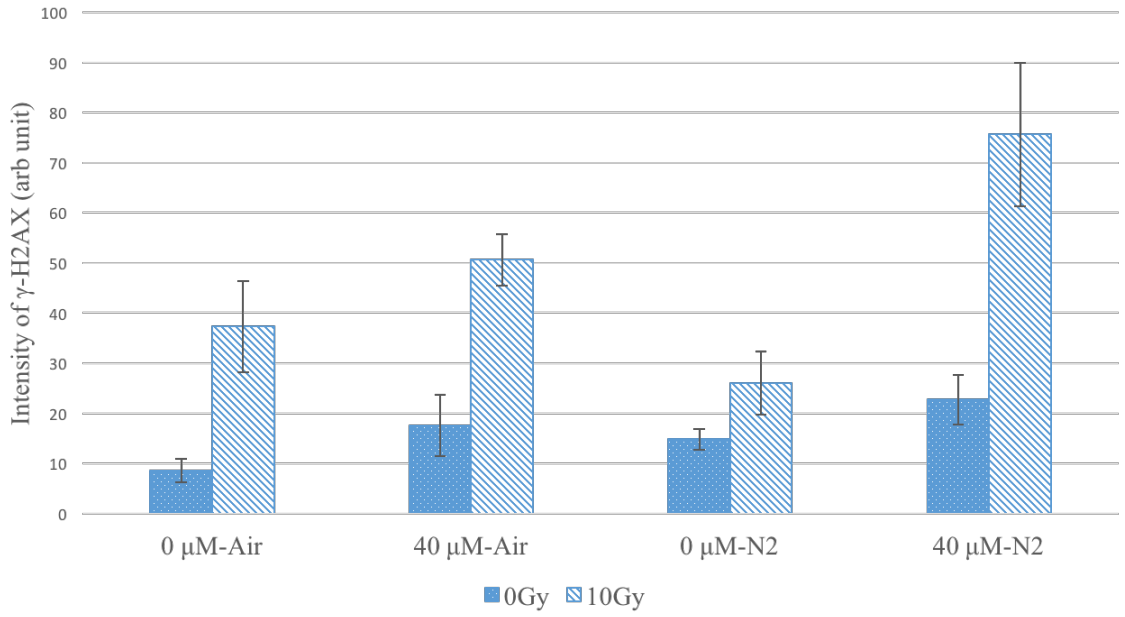

Figure 3-3. γ-H2AX DNA DSBs detection in A549 cancer cells treated by the FMD compound combined with X-ray radiation. A549 human lung cancer cells were treated with/without 40 μM of FMD compound for 8 hours, followed by 0/10Gy X-Ray radiation in normoxia/hypoxic environment. 2 days after irradiation, γ-H2AX DNA DSBs detection assay was performed. The intensity of γ-H2AX is proportional to the yield of DSBs per cell.

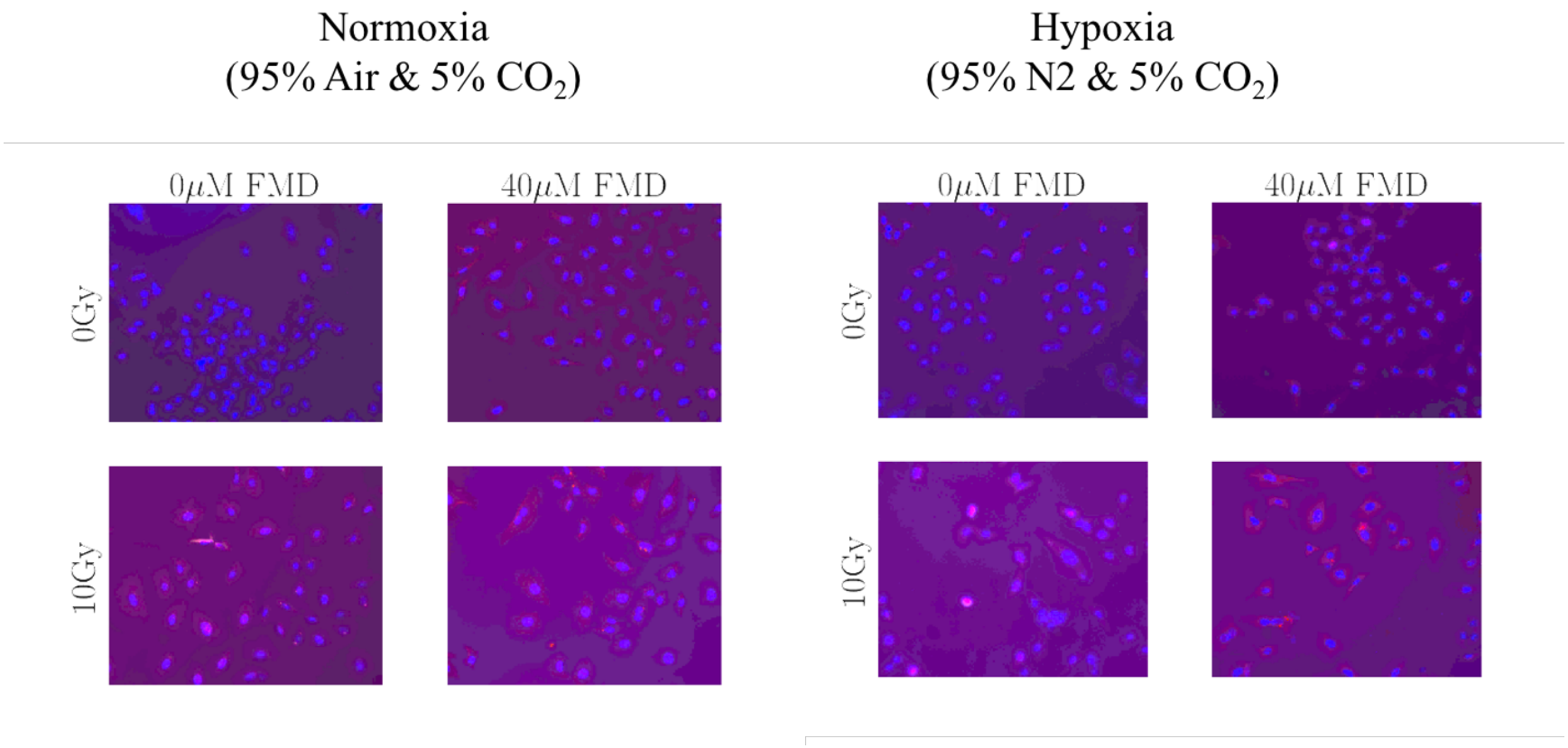

Figure 3-4. Image of X-radiation-induced genotoxicity of FMD compound in A549 human lung cancer cells using the HCS DNA Damage Kit. A549 cells were treated with 40 μM FMD compound for 8 hours. During this period, the normoxia cells were incubated at 37 ℃, 95% Air, 5% CO_2, while the hypoxia cells were incubated at 37 ℃, 95% Air, 5% CO_2 for 6 hours and 37 ℃, 95% N_2, 5% CO_2 for 2 hours.

3.4 Conclusion

In this experiment, it was confirmed that the FMD compound is a sensitive DNA damaging agent under IR. The proposed mechanism is described as the following:

- In the normoxic environment, the e_{pre}^-, which was generated from the radiolysis of water, was either absorbed by an oxygen molecule to form the a $O_2^{\bullet -}$, or dissociatively attached to the a FMD molecule to form FMD radical fragments. However, the $O_2^{\bullet -}$ is less effective in creating DNA DSBs compared to the FMD radical fragments. The high level of oxygen in the normoxic environment will lead to the loss of effectiveness of FMD compound.

$$e_{pre}^- + O_2 + FMD \rightarrow O_2^{\bullet -} + FMD^{\bullet -} \rightarrow \text{Activated FMD} \rightarrow \text{DNA Damages} \qquad \textit{Eq. 3-1}$$

- In the hypoxic environment, there were more e_{pre}^- that can dissociatively attached to FMD molecules, the activation of the FMD compound consequently lead to the increase of the yield of DNA DSBs.

$$e_{pre}^- + FMD \rightarrow FMD^{\bullet -} \rightarrow \text{More Activated FMD} \rightarrow \text{More DNA Damages} \qquad \textit{Eq. 3-2}$$

We therefore conclude that, FMD compound has moderate genotoxicity in the absence of radiation; however, when combined with IR, FMD compound is highly effective in producing DNA damages, especially DNA DSBs, in hypoxic cancer cells.

Chapter 4 Activated caspase assay of apoptosis measurement

4.1 Introduction

DNA damages could lead to programmed cell death, namely, apoptosis, pyroptosis, and necroptosis. Caspases are key components in the molecular identification of this intracellular suicide program[81]–[83]. During the process of programmed cell death, the activation of caspase enzymes will keep any impact on the surrounding tissues to a minimum[84]. Caspase deficiency has been reported as a inducement for tumor initiation[85], on the contrary, the over activation of caspase may result in neurodegenerative diseases, such as Alzheimer's disease (AD)[86].

One of the most distinctive features of early stage of apoptosis is the activation of caspases. There are two major pathways for the activation of caspase. 1) the cell surface death receptor pathway[87] and 2) the mitochondria initiated pathway. In the death receptor pathway, the activation of caspase 8 aids in the cleavage of the downstream protein, Bid (BH3 interacting-domain death agonist) protein, and the activation of the downstream caspase, caspase 3. In the mitochondria initiated pathway, the activated caspase 9 can activate downstream caspases, caspase 3, 6, and 7. It was also reported that there exists cross-talk between these two pathways[88]. Caspase 3 is considered as the convergence point of these two signalling pathways, as caspase 3 can be activated either by caspase 8 or 9. Therefore, the detection of

the activated caspase 3 provided us a reliable and convenient approach to monitor the apoptosis process.

To detect the activation of caspase 3, molecular probes consisting of a short peptide, DEVD, and a DNA binding dye were added into the tested cell. As shown Figure 4-1,when apoptosis starts, the activated caspase 3 will cleave the linkage between DEVD and the DNA binding dye[89]. Therefore, the DNA binding dye will be released by caspase 3. The released dye will bind to DNA, and emit green florescence after excitation. Eventually, apoptosis can be quantified via immunofluorescence microscope.

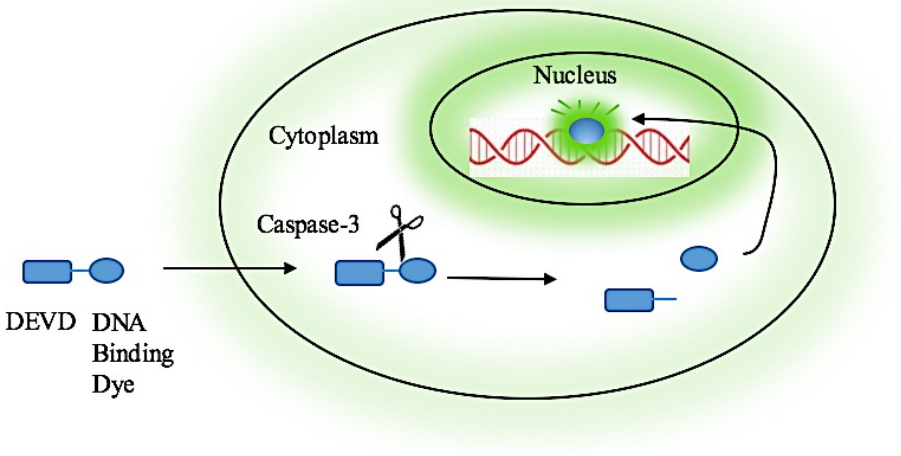

Figure 4-1. The schematic illustration of the working mechanism of the Caspase 3 detection probes. The activation of caspase 3 represents the apoptosis process of the cell death. The detection probe is consisted with a short peptide, DEVD, linked to a DNA binding dye. Activated caspase 3 can cleave the linkage and release the dye. The released dye can then bind to DNA and emit a bright green florescence after excitation.

4.2 Method

4.2.1 Cell culture

The human cervical cancer cells, HeLa (ATCC® CCL-2™) were directly purchased from the American type culture collection (ATCC). Cells were grown in Eagles Minimum Essential Medium (MEM) containing 10% fetal bovine serum (Invitrogen) and 1% penicillin-streptomycin (PS) solution (ATCC® 30-2300™). The cells were incubated at 37 ℃ in a regular CO_2 incubator, CO_2 level was maintained at 5%, and relative humidity was maintained at 10%. The cells were passaged twice a week.

4.2.2 Radiation treatment

The radiation treatment is almost the same as it has been described in the previous chapter. The HeLa cells in the logarithmic growth phase were seeded in black 96-well plates at a density of 2000 cells/well. 0/4/8 μM of FMD compound were added with fresh medium after 24 hours of seeding. Then, the normoxic cells were incubated in a regular incubator for 8 hours; while the hypoxic cells were incubated in a regular incubator for 6 hours and then sealed in the hypoxic environment system for 2 hours (as described in last chapter). Following that, 0/5/10 Gy of X-ray (Precision, X-RAD IR225) were applied to these cells at a dose rate of 2.5 Gy/mins. After radiation, both of the normoxic cells and the hypoxic cells were incubated in a regular cell incubator for 2 days for the final detection of activated caspase.

4.2.3 Caspase detection kit

CellEvent™ Caspase-3/7 Green Detection Reagent (Invitrogen, Catalog # C10423) was used for the detection of activated caspase. The kit was used following the protocol provided by the manufacturing company without further modification. In brief, the cells were treated with different doses of FMD compound and X-ray radiation in normoxia/hypoxia conditions, 2 days after radiation, the cells were incubated with CellEvent™ Caspase-3/7 Green Detection Reagent (2 μM) for half an hour in normal incubation condition. The pictures of the cells were taken via a Nikon Eclipse TS1000 microscope. The apoptotic cells can be excited at 502 nm, and the emission is 530 nm. The number of apoptotic cells were then counted by eyes. The percentage of cells with activated caspase is defined as the ratio of the number of apoptotic cells to the total number of cells.

4.3 Result

The images for the apoptosis analysis in the treated human cervical cancer cells (HeLa) were shown in Figure 4-3. The cells with green emission were apoptotic cells, and the green emission was from the activation of caspase 3. In the absence of radiation, as the concentration of the FMD compound increased, there was an increase in the percentage of apoptotic cells. This result suggests that the FMD compound has intrinsic cytotoxicity. In the presence of the FMD compound, the percentage of apoptotic cells was increased with radiation dose, this result shows that the FMD compound indeed has radiosensitivity.

The quantitative analyses of these figures were provided in Figure 4-2. It can be seen that in the absence of the FMD compound, after being exposed to 10Gy X-ray radiation, 19.5±2.0 % of apoptotic cells were observed in normoxia condition, but only 12.1±1.2 % were observed in hypoxia condition. The reduction of the IR induced apoptosis in hypoxia condition showed consistency with our previous DNA DSBs observation. Not surprisingly, cancer cells showed resistance to radiation in the hypoxic environment. However, by comparing the percentages of apoptosis between the radiated cells treated with/without FMD compound, one can see that with 8 μM of the FMD compound, the percentage of apoptosis was increased both in normoxia and hypoxia conditions. The increase in hypoxia condition (5-folds increment) was significantly higher than that in normoxia condition (2-fold increment).

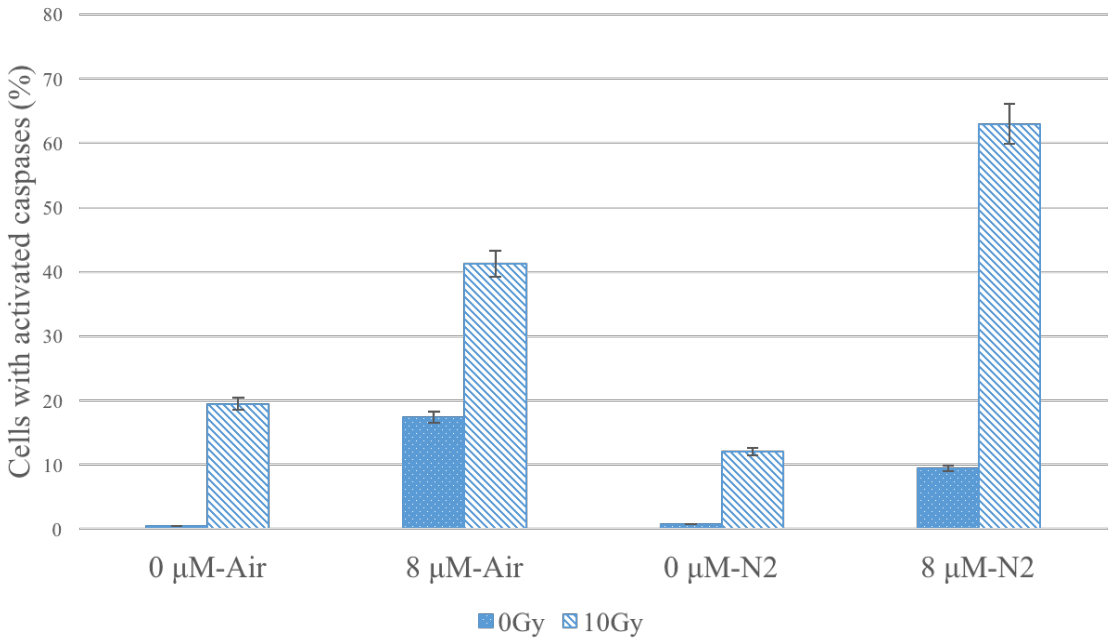

Figure 4-2. The quantitative measurements of apoptosis in human cervical cancer cells (HeLa) treated by 0/8 μM of the FMD compound with 0/10Gy of X-ray radiation under normoxia/hypoxia conditions. The percentage of cells with activated caspases, the ratio of the number of cells with green fluorescence to the total number of cells in an image, represents the percentage of apoptotic cells in the whole population.

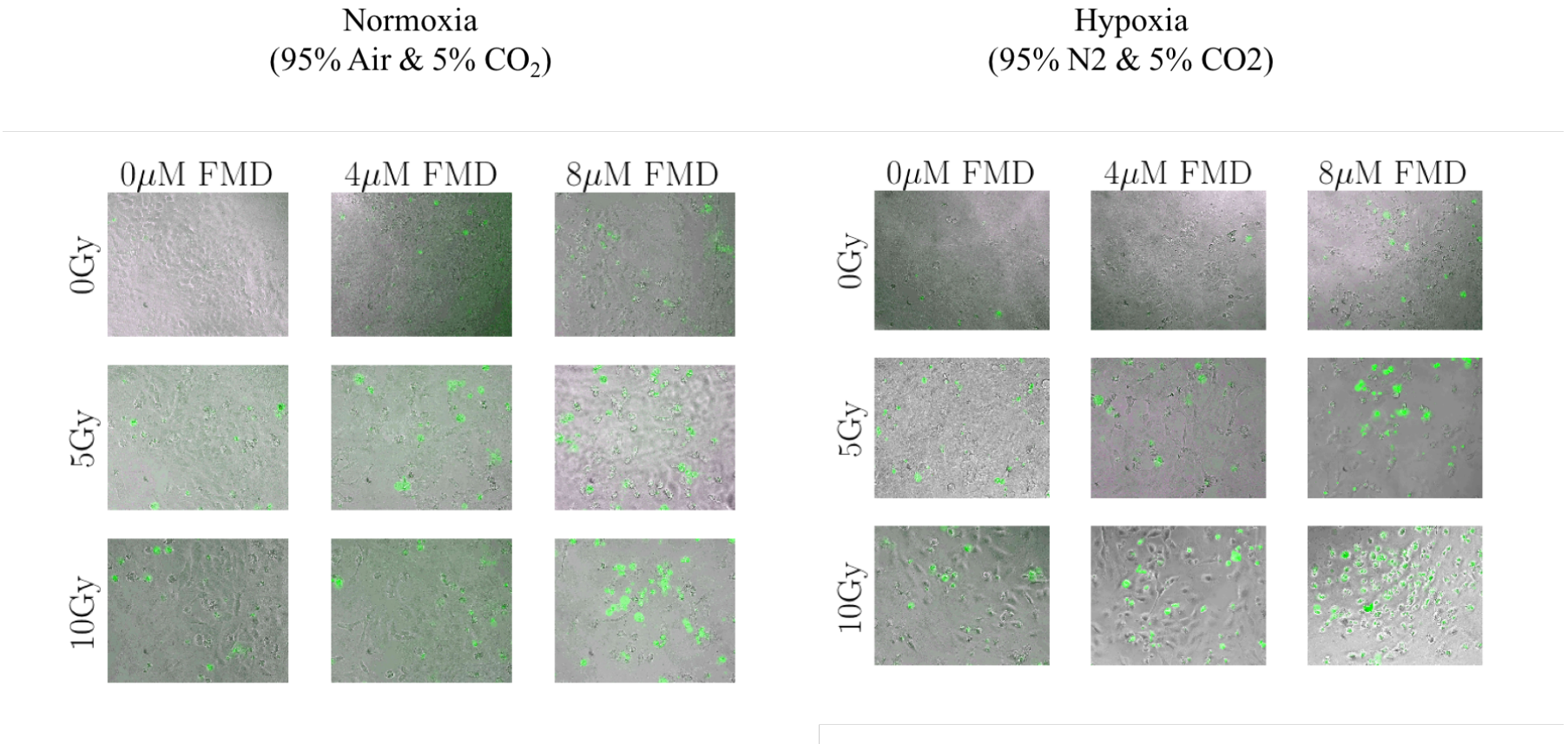

Figure 4-3. Images of the human cervical cancer cells with activated caspase. Hela cells were treated with 0/4/8 μM of the FMD compound followed by 0/5/10 Gy of X-ray radiation. At 2 days' post-irradiation, the caspase detection reagent was added. The apoptosis in Hela cells were represented by green fluorescence. The cells on the left panels were irradiated under normoxia condition, the cells on the right panels were irradiated under hypoxia condition.

4.4 Conclusion

In this experiment, it was proved that the FMD compound has radiosensitivity that can increase apoptosis in human cancer cells. It was also proved that the radiosensitivity was increased by the hypoxic gas environment but limited by the normoxic gas environment. The proposed mechanism is described as the following:

- In the normoxia condition, the excess of oxygen will limit the attachment of the pre-solvated electrons and the FMD molecules. Only a limited number of FMD molecules could be activated in the presence of oxygen.

$$e^-_{pre} + O_2 + FMD \rightarrow O_2^{\bullet -} + FMD^{\bullet -} \rightarrow \text{Activated FMD} \rightarrow \text{Apoptosis} \qquad \textit{Eq. 4-1}$$

- In the hypoxia condition, the FMD molecules have more chance to be dissociatively attached by a pre-solvated electron. The dissociated FMD fragments were efficient in increasing apoptosis. Therefore, the FMD compound's radiosensitizing effect is more significant in the absence of oxygen.

$$e^-_{pre} + O_2 + FMD \rightarrow O_2^{\bullet -} + FMD^{\bullet -} \rightarrow \text{Activated FMD} \rightarrow \text{More Apoptosis} \qquad \textit{Eq. 4-2}$$

Chapter 5 Clonogenic assay

5.1 Introduction

Clonogenic assay and MTT assay are the two most popular *in vitro* techniques to evaluate the potency of anticancer agents. Clonogenic assay is widely used to determine the proliferation and survival of the irradiated cancer cells, while the MTT assay is commonly used to evaluate the cancer cell variability (metabolic activity) after treated with cytotoxicity molecules[90].

In radiobiology, for the proliferating cells, if a cell lost its ability to proliferate infinitely and cannot produce a large number of offsprings, this cell is considered as dead. The clonogenic assay is to test the capability of a single cell to proliferate into a large colony. Generally, the clonogenic assay is composed of five steps: cell preparation, cell treatment, plating, staining, and counting (more details will be given in the method section). A colony can be recognized by naked eyes are of at least 50 cells[91]. The MTT assay is a colorimetric assay, the cells with metabolic activities can reduce MTT to formazan crystal, a purple-colored product. The quantity of formazan formed can represent the cell's variability. The MTT assay is a fast and inexpensive test, but it is not able to directly get access to the cytocidal activity and the number of cells[92]. More importantly, the metabolic states between normoxic cells and hypoxic cells are different. The difference in metabolic states result in the fact that the MTT results cannot be crosswisely compared between normoxic and hypoxic groups.

Therefore, in order to determine if the FMD compound can efficiently decrease the cancer cells' survival when combined with radiation, and to compare the sensitizing effect between hypoxia and normoxia, clonogenic assay, rather than MTT assay, should be conducted in this experiment.

5.2 Method

5.2.1 Cell culture

A549 human lung cancer cells were used in this experiment. Cell line information and cell culture conditions are identical with Chapter 3.

5.2.2 Radiation treatment

The flow chart of the cell treatment can be seen in Figure 5-1. The logarithmic phase A549 cells were seeded in 6-well plates at various densities as shown in Table 5-1. First, the cells were incubated regularly at 37 ℃, 5% CO_2, 95% Air, for 24 hours. Then different concentrations of the FMD compound were added to these 6-well plates, the normoxic cells were then incubated in incubator for 8 hours, while the hypoxic cells were incubated in incubator for 6 hours, and then sealed in the hypoxic environment system (37 ℃, 5% CO_2, 95% N_2) for 2 hours. Then different doses of X-ray were applied to these plates. After irradiation, cells were incubated in incubator at 37 ℃, 5% CO_2, 95% Air for 16 days to form colonies. The colonies were then washed by PBS, stained by the mixture of crystal violet and glutaraldehyde for half an hour. Finally, the plates were washed by tap water, and the colonies were counted by naked eyes.

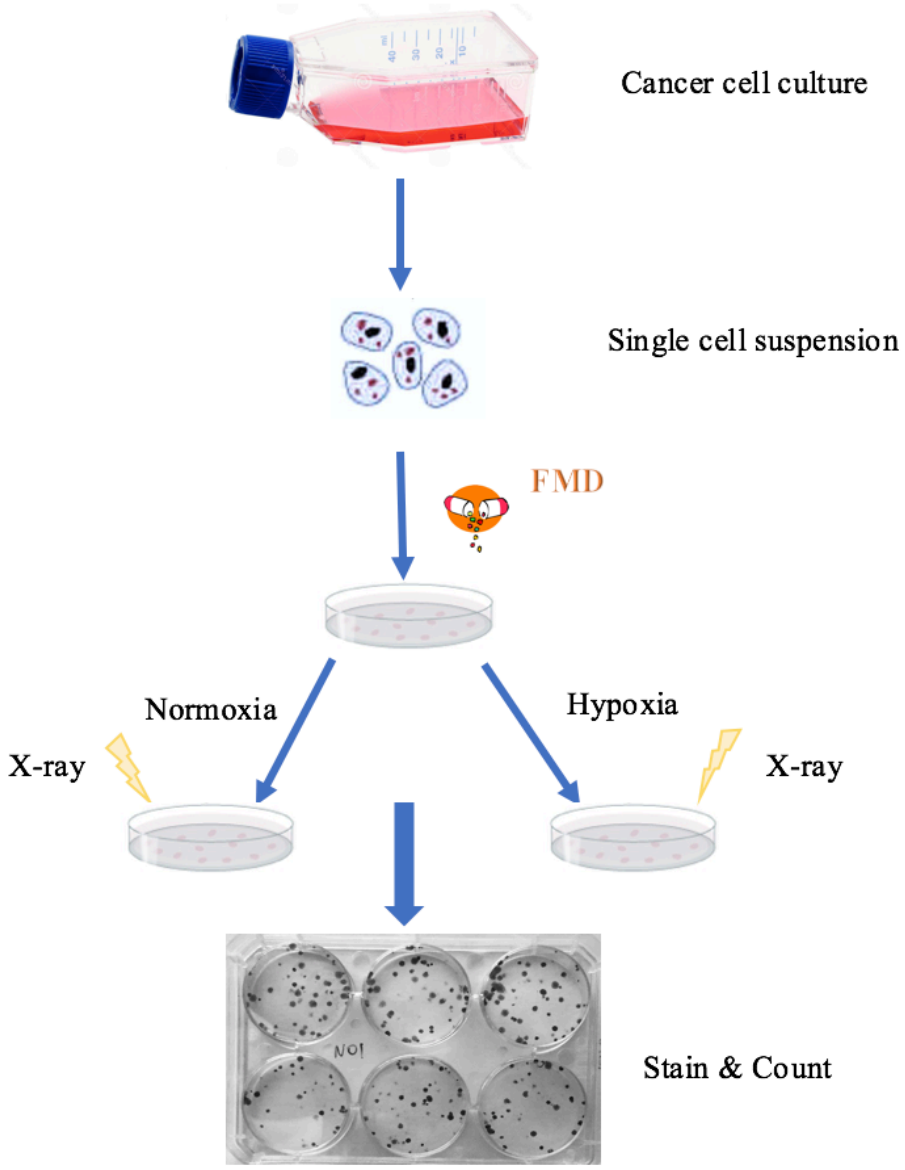

Figure 5-1. The flow chart of the clonogenic assay. Cancer cells were harvested and trypsinized to signal cell suspension. Then the density of the cell suspension was measured by a hemocytometer. Different numbers of cells were seeded in 6-well plates depend on the treatments. FMD compoumd was added 8 hours prior to radiation. Hypoxic condition was achieved by sealing the plates in our hypoxic environment system. The colonies were stained and counted after 16 days' post-irradiate incubation.

Seed Cell Number	*0Gy*	*2.5Gy*	*5Gy*	*7.5Gy*	*10Gy*
0 μM -N_2	100	400	400	1000	4000
20 μM -N_2	100	400	600	1500	6000
40 μM -N_2	100	400	600	1500	6000
0 μM -Air	100	500	750	1500	6000
20 μM -Air	100	500	1000	2000	6000
40 μM -Air	100	500	1000	2000	6000

Table 5-1. The number of seeded A549 human lung cancer cells in the clonogenic assay.

5.3 Result

In order to determine if the FMD compound can improve the effect of radiation therapy by decreasing the cancer cells' survival, human lung cancer cells (A549) were seeded in 6-well plates, treated with 0/20/40 μM of the FMD compound with 0-10 Gy of X-ray under normoxia/hypoxia conditions. As the result shown in Figure 5-2, the survival rate of the cancer cells is decreasing with the X-ray dose increasing. In the presence of FMD compound, the cell killing was enhanced both in normoxia and hypoxia conditions. This result is consistent with our previous DNA damage measurements and apoptosis measurements. For the control groups, the oxygen enhancement effect can also be observed from Figure 5-2, this is a justification for our hypoxic environment system's validation.

To compare the radiosensitivities of the FMD compound under hypoxic environment and normoxic environment, the radio enhancement ratio (ER) of the FMD compound for both of these two situations were calculated. The ER is defined as the ratio of the radiation dose required to achieve a certain survival rate over that in the presence of radiosensitizer (see Eq. 5-1). As shown in Figure 5-3, at 20% survival rate, the ER for hypoxic cell was 1.42 ± 0.05, the ER for the normoxic cell was 1.10 ± 0.05. The radiosensitizing effect of the FMD compound in hypoxic environment was predominantly enhanced.

$$ER = \frac{\text{Dose for producing a given survial fraction}}{\text{Dose for produce the same level of survival fraction with FMD}} \qquad \textit{Eq. 5-1}$$

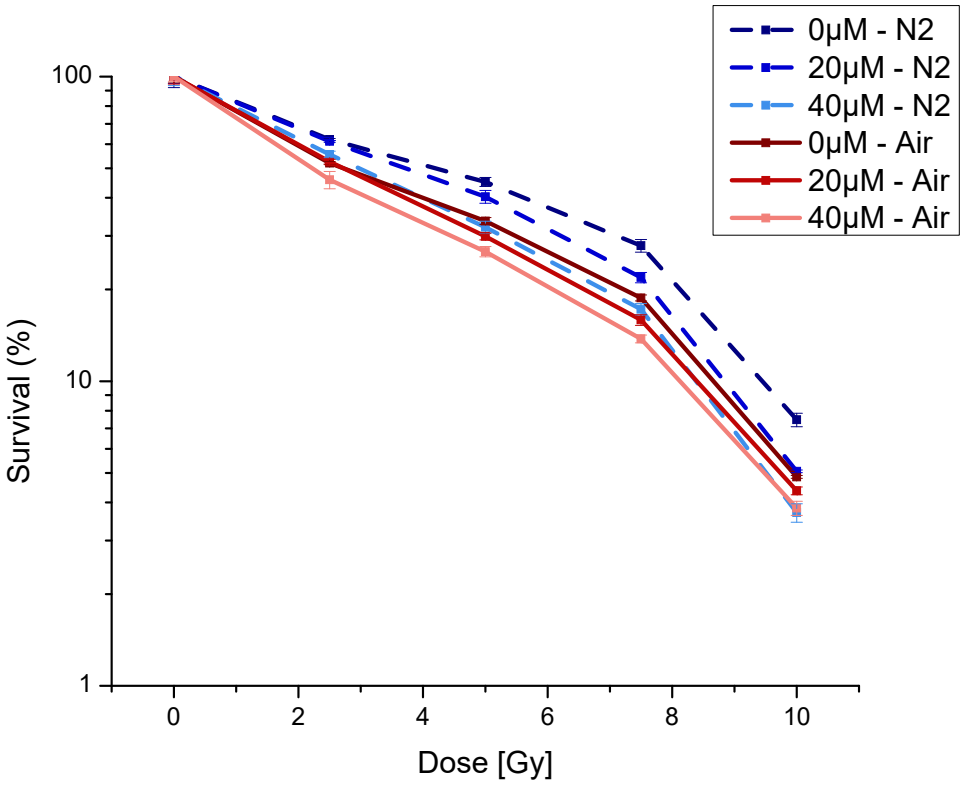

Figure 5-2. *In vitro* clonogenic assay of the radiosensitizing effects of the FMD compound tested in human lung cancer cells (A549). The blue dashed lines are the survival curves for the cancer cells, which were in hypoxic environment during IR; the red solid lines are the survival curves for the cancer cells which were in normoxic environment during IR.

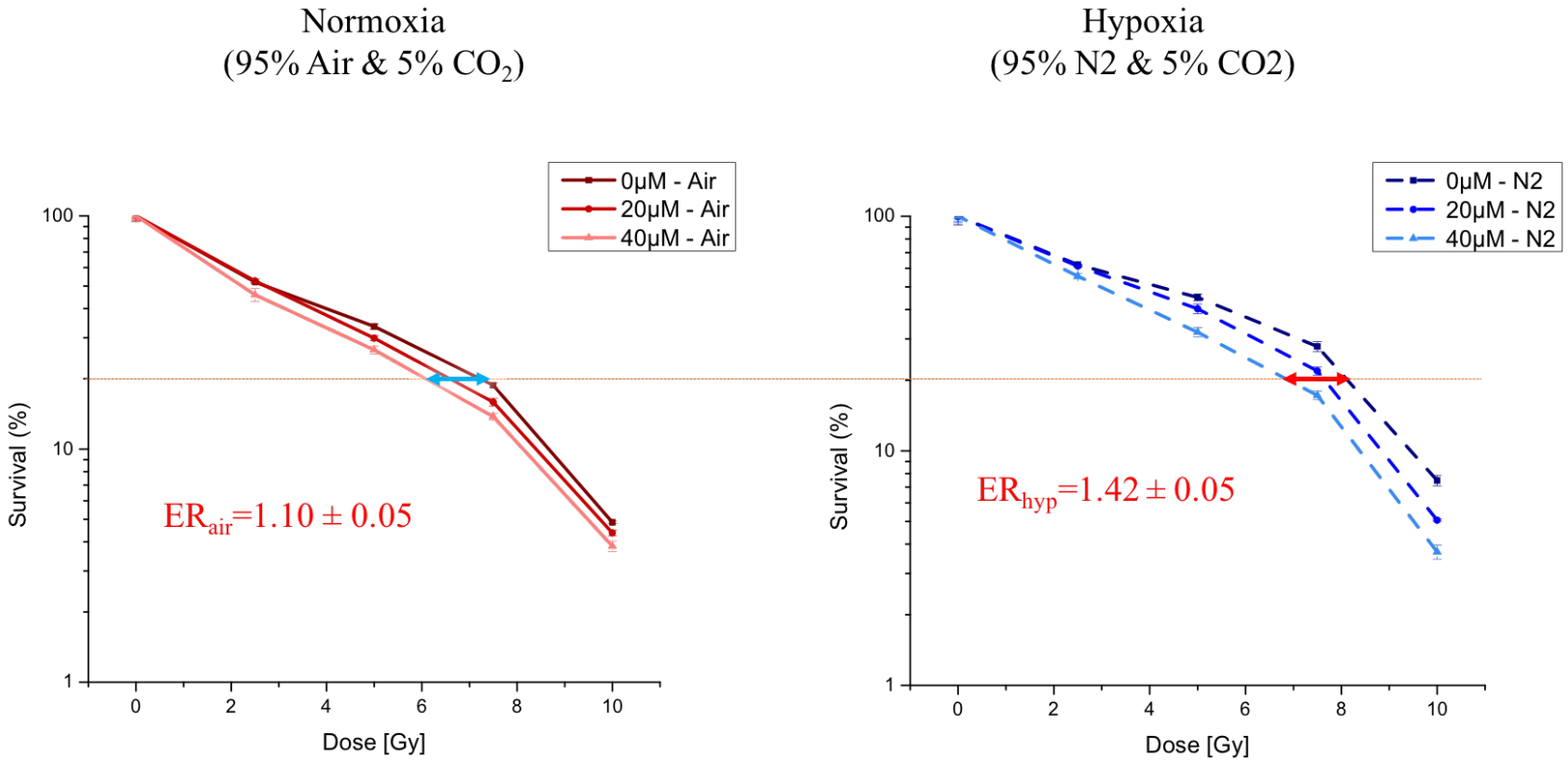

Figure 5-3. *In vitro* clonogenic assay of the radiosensitizing effects of the FMD compound tested in human lung cancer cells (A549). The left panel shows the survival rates of cancer cells irradiated under normoxia condition, the right panel shows the survival rates of cancer cells irradiated under hypoxia conditions. The radio enhancement ratio (ER) for the right panel is significantly greater than that in the left panel.

5.4 Conclusion

In this experiment, the radiosensitivity of the FMD compound was tested in human lung cancer cells (A549). The survival curves were reduced in the presence of FMD compound combined with radiation, the results confirmed that the FMD compound has radiosensitivity both in the normoxic and hypoxic environment.

By comparing the radio enhancement ratios in both of these two conditions, it can be found that the radiosensitivity of the FMD compound was significantly enhanced in the hypoxic environment. These results are consistent with the observation from the *in vitro* DNA DSBs experiments and the *in vitro* apoptosis experiments. We therefore conclude that in the absence of oxygen molecules, more FMD molecules will be activated by e_{pre}^-, and the activated FMD radical fragments are efficient in producing DNA DSBs and therefore apoptosis will be enhanced. This may directly lead to the decline of cancer cells' survival rates. In the presence of molecular oxygen, the formation of $O_2^{\bullet -}$, will partially hamper the effectiveness of the FMD compound and therefore, the radiosensitivity of the FMD compound in normoxic cells will be limited. The enhancement ratio of the FMD compound in hypoxic environment is 1.42 ± 0.05, which is noticeably larger than the enhancement ratio in normoxic environment (1.10 ± 0.05). These results suggest that the FMD compound has unique features that can be selectively activated in the hypoxic environment, and has

promising potential to be applied clinically to overcome the hypoxia-mediated radioresistance of a variety of cancer cells.

Chapter 6 Summary

In summary, by conducting various *in vitro* experiments, we have demonstrated that FMD compound is an effective radiosensitizer on hypoxic human cancer cell lines. The radiosensitizing effect could be enhanced by the presence of hypoxia in the microenvironment of tumor. The experiment also demonstrates that the limited radiosensitivity of the FMD compound in the normoxic environment/tissue was a consequence of deficient pre-solvated electrons to activate the FMD. Our results have revealed a mechanism explaining the radiosensitizing effect of a variety of pre-solvated electron activated radiosensitizers that are effective in the hypoxic tumor environment.

The *in vitro* steady-state absorption spectra analyses have shown that there exists a competition binding of pre-solvated electrons between oxygen and FMD molecules. The *in vitro* DNA DSBs detection experiment further indicates that in the absence of oxygen, the pre-hydrated electrons produced by ionizing radiation (IR) of water, attach to our FMD molecules and initiate a series of dissociative electron transfer (DET) reactions, thus induce severe DNA damage, especially double strand breaks. Meanwhile, under normoxia circumstance, oxygen molecules preferentially capture pre-solvated electrons to form superoxide radicals, which are relatively moderate and less destructive comparing with radicals formed from the dissociation of FMD molecules. Consequently, in the presence of oxygen, DNA is partially detoxified by the FMD compound during IR. The *in vitro* hypoxia-activated radiosensitivity of the FMD compound has been evaluated through

immunofluorescence and clonogenic assays. The results have confirmed that the FMD compound can decrease the cancer cells' survival rate and increase the number of apoptotic cells predominately in hypoxic environment.

These findings have provided a new understanding of the mechanism of the FMD compound acting as a hypoxia-activated radiosensitizer and have highlighted a potential application of our FMD agent in natural targeted radiotherapies. The results might be helpful to exploit pre-solvated electrons for novel cancer therapies.

References

[1] R. L. Siegel, K. D. Miller, and A. Jemal, "Cancer statistics, 2016," *CA. Cancer J. Clin.*, vol. 66, no. 1, pp. 7–30, 2016.

[2] W. H. Organization, "GLOBOCAN 2012: Estimated cancer incidence, mortality and prevalence worldwide in 2012," *Lyon, Fr. Int. Agency Res. Cancer*, 2014.

[3] D. Carter, "New global survey shows an increasing cancer burden.," *Am. J. Nurs.*, vol. 114, no. 3, p. 17, 2014.

[4] A. Mullard, "2014 FDA drug approvals," *Nat. Rev. Drug Discov.*, vol. 14, no. 2, pp. 77–81, 2015.

[5] B. D. Buffery, "Innovation tops current trends in the 2016 oncology drug pipeline," *Am. Heal. drug benefits*, vol. 9, no. 4, pp. 233–238, 2016.

[6] D. Buffery, "The 2015 oncology drug pipeline: innovation drives the race to cure cancer," *Am. Heal. drug benefits*, vol. 8, no. 4, p. 216, 2015.

[7] B. Hughes, "2009 FDA drug approvals.," *Nat. Rev. Drug Discov.*, vol. 9, pp. 89–92, 2010.

[8] A. Mullard, "2013 FDA drug approvals.," *Nat. Rev. Drug Discov.*, vol. 13, pp. 85–89, 2014.

[9] S. Mailankody and V. Prasad, "Five years of cancer drug approvals: innovation, efficacy, and costs," *JAMA Oncol.*, vol. 1, no. 4, pp. 539–540, 2015.

[10] M. O'Dell and M. Stubblefield, *Cancer Rehabilitation: Principles and Practice*. 2009.

[11] J. B. Gibbs, "Mechanism-Based Target Identification and Drug Discovery in Cancer Research," *Science (80-.).*, vol. 287, no. 5460, pp. 1969–1973, 2000.

[12] J. Walter, *Cancer and radiotherapy: a short guide for nurses and medical students*. Churchill Livingstone, 1977.

[13] C. Von Sonntag, *The chemical basis of radiation biology*. Taylor & Francis London, 1987.

[14] T. Ito, "Dependence of the Yield of Strand Breaks Induced by γ-rays in DNA on the Physical Conditions of Exposure: Water Content and Temperature," *Int. J. Radiat. Biol.*, vol. 63, no. 3, 1993.

[15] G. C. Barnett, C. M. L. West, A. M. Dunning, R. M. Elliott, C. E. Coles, P. D. P. Pharoah, and N. G. Burnet, "Normal tissue reactions to radiotherapy: towards tailoring treatment dose by genotype," *Nat. Rev. Cancer*, vol. 9, no. 2, pp. 134–142, 2009.

[16] C.-R. Wang, J. Mahmood, Q.-R. Zhang, A. Vedadi, J. Warrington, N. Ou, R. G. Bristow, D. A. Jaffray, and Q.-B. Lu, "In Vitro and In Vivo Studies of a New Class of Anticancer Molecules for Targeted Radiotherapy of Cancer," *Mol. Cancer Ther.*, vol. 15, no. 4, pp. 640–650, 2016.

[17] H. Lodish, D. Baltimore, A. Berk, S. L. Zipursky, P. Matsudaira, and J. Darnell, *Molecular cell biology*, vol. 3. Scientific American Books New York, 1995.

[18] R. J. Woods and A. K. Pikaev, *Applied radiation chemistry: radiation processing*. John Wiley & Sons, 1994.

[19] S. Le Caër, "Water radiolysis: influence of oxide surfaces on H2 production under ionizing radiation," *Water*, vol. 3, no. 1, pp. 235–253, 2011.

[20] C. M. Lousada, I. L. Soroka, Y. Yagodzinskyy, N. V Tarakina, O. Todoshchenko, H. Hänninen, P. A. Korzhavyi, and M. Jonsson, "Gamma radiation induces hydrogen absorption by copper in water," *Sci. Rep.*, vol. 6, 2016.

[21] Q.-B. Lu, "Effects and applications of ultrashort-lived prehydrated electrons in radiation biology and radiotherapy of cancer," *Mutat. Res. Mutat. Res.*, vol. 704, no. 1, pp. 190–199, 2010.

[22] J. F. Wishart 1958- and D. G. Nocera 1957-, Eds., *Photochemistry and radiation chemistry complementary methods for the study of electron transfer*. Washington, DC: American Chemical Society, 1998.

[23] J. A. LaVerne and R. H. Schuler, “Decomposition of water by very high linear energy transfer radiations,” *J. Phys. Chem.*, vol. 87, no. 23, pp. 4564–4565, 1983.

[24] T. Luo, J. Yu, J. Nguyen, C.-R. Wang, R. G. Bristow, D. A. Jaffray, X. Z. Zhou, K. P. Lu, and Q.-B. Lu, “Electron transfer-based combination therapy of cisplatin with tetramethyl-p-phenylenediamine for ovarian, cervical, and lung cancers,” *Proc. Natl. Acad. Sci.*, vol. 109, no. 26, pp. 10175–10180, 2012.

[25] J. Nguyen, Y. Ma, T. Luo, R. G. Bristow, D. A. Jaffray, and Q.-B. Lu, “Direct observation of ultrafast-electron-transfer reactions unravels high effectiveness of reductive DNA damage,” *Proc. Natl. Acad. Sci.*, vol. 108, no. 29, pp. 11778–11783, 2011.

[26] C.-R. Wang, T. Luo, and Q.-B. Lu, “On the lifetimes and physical nature of incompletely relaxed electrons in liquid water,” *Phys. Chem. Chem. Phys.*, vol. 10, no. 30, pp. 4463–4470, 2008.

[27] J. W. Boag and E. J. Hart, “ABSORPTION SPECTRA IN IRRADIATED WATER AND SOME SOLUTIONS. PART I. ABSORPTION SPECTRA OF’HYDRATED'ELECTRON,” *Nature*, vol. 197, 1963.

[28] J. M. Wiesenfeld and E. P. Ippen, “Dynamics of electron solvation in liquid water,” *Chem. Phys. Lett.*, vol. 73, no. 1, pp. 47–50, 1980.

[29] W. J. Chase and J. W. Hunt, “Solvation time of the electron in polar liquids. Water and alcohols,” *J. Phys. Chem.*, vol. 79, no. 26, pp. 2835–2845, 1975.

[30] D. P. Millar, R. Shah, and A. H. Zewail, “Picosecond saturation spectroscopy of cresyl violet: rotational diffusion by a ‘sticking’ boundary condition in the liquid phase,” *Chem. Phys. Lett.*, vol. 66, no. 3, pp. 435–440, 1979.

[31] N. F. Scherer, J. L. Knee, D. D. Smith, and A. H. Zewail, “Femtosecond photofragment spectroscopy of the reaction iodine cyanide (ICN). fwdarw. cyanogen (CN)+ atomic iodine,” *J. Phys. Chem.*, vol. 89, no. 24, pp. 5141–5143, 1985.

[32] A. Migus, Y. Gauduel, J. L. Martin, and A. Antonetti, “Excess electrons in liquid

water: first evidence of a prehydrated state with femtosecond lifetime," *Phys. Rev. Lett.*, vol. 58, no. 15, p. 1559, 1987.

[33] D. W. Siemann, "The unique characteristics of tumor vasculature and preclinical evidence for its selective disruption by Tumor-Vascular Disrupting Agents," *Cancer Treat. Rev.*, vol. 37, no. 1, pp. 63–74, 2011.

[34] M. A. Konerding, E. Fait, and A. Gaumann, "3D microvascular architecture of pre-cancerous lesions and invasive carcinomas of the colon," *Br. J. Cancer*, vol. 84, no. 10, p. 1354, 2001.

[35] T. P. Padera, A. Kadambi, E. di Tomaso, C. M. Carreira, E. B. Brown, Y. Boucher, N. C. Choi, D. Mathisen, J. Wain, and E. J. Mark, "Lymphatic metastasis in the absence of functional intratumor lymphatics," *Science (80-.).*, vol. 296, no. 5574, pp. 1883–1886, 2002.

[36] C. Riva, C. Chauvin, C. Pison, and X. Leverve, "Cellular physiology and molecular events in hypoxia-induced apoptosis.," *Anticancer Res.*, vol. 18, no. 6B, pp. 4729–4736, 1997.

[37] R. H. Thomlinson and L. H. Gray, "The histological structure of some human lung cancers and the possible implications for radiotherapy," *Br. J. Cancer*, vol. 9, no. 4, p. 539, 1955.

[38] T. G. Graeber, C. Osmanian, T. Jacks, D. E. Housman, C. J. Koch, S. W. Lowe, and A. J. Giaccia, "Hypoxia-mediated selection of cells with diminished apoptotic potential in solid tumours," *Nature*, vol. 379, no. 6560, pp. 88–91, 1996.

[39] C. Y. Kim, M. H. Tsai, C. Osmanian, T. G. Graeber, J. E. Lee, R. G. Giffard, J. A. DiPaolo, D. M. Peehl, and A. J. Giaccia, "Selection of human cervical epithelial cells that possess reduced apoptotic potential to low-oxygen conditions," *Cancer Res.*, vol. 57, no. 19, pp. 4200–4204, 1997.

[40] G. L. Wang, B.-H. Jiang, E. A. Rue, and G. L. Semenza, "Hypoxia-inducible factor 1 is a basic-helix-loop-helix-PAS heterodimer regulated by cellular O2 tension," *Proc.*

Natl. Acad. Sci., vol. 92, no. 12, pp. 5510–5514, 1995.

[41] T. Y. Reynolds, S. Rockwell, and P. M. Glazer, "Genetic instability induced by the tumor microenvironment," *Cancer Res.*, vol. 56, no. 24, pp. 5754–5757, 1996.

[42] J. B. Mitchell, S. McPherson, W. DeGraff, J. Gamson, A. Zabell, and A. Russo, "Oxygen dependence of hematoporphyrin derivative-induced photoinactivation of Chinese hamster cells," *Cancer Res.*, vol. 45, no. 5, pp. 2008–2011, 1985.

[43] E. J. Hall and A. J. Giaccia, "The oxygen effect and reoxygenation," *Radiobiol. Radiol.*, vol. 6, pp. 85–105, 1994.

[44] I. Tannock and R. P. Hill 1942-, Eds., *The Basic science of oncology*, 2nd ed. CN. New York: McGraw-Hill, Health Professions Division, 1992.

[45] J. K. Mohindra and A. M. Rauth, "Increased cell killing by metronidazole and nitrofurazone of hypoxic compared to aerobic mammalian cells," *Cancer Res.*, vol. 36, no. 3, pp. 930–936, 1976.

[46] D. J. Chaplin, M. R. Horsman, M. J. Trotter, and D. W. Siemann, "Therapeutic significance of microenvironmental factors," *Blood Perfus. Microenviron. Hum. Tumors*, pp. 131–143, 1998.

[47] M. Höckel and P. Vaupel, "Tumor hypoxia: definitions and current clinical, biologic, and molecular aspects," *J. Natl. Cancer Inst.*, vol. 93, no. 4, pp. 266–276, 2001.

[48] M. S. Soengas, R. M. Alarcon, H. Yoshida, R. Hakem, T. W. Mak, and S. W. Lowe, "Apaf-1 and caspase-9 in p53-dependent apoptosis and tumor inhibition," *Science (80-.).*, vol. 284, no. 5411, pp. 156–159, 1999.

[49] C. V Dang and G. L. Semenza, "Oncogenic alterations of metabolism," *Trends Biochem. Sci.*, vol. 24, no. 2, pp. 68–72, 1999.

[50] B. A. Teicher, S. A. Holden, A. Al-Achi, and T. S. Herman, "Classification of antineoplastic treatments by their differential toxicity toward putative oxygenated and hypoxic tumor subpopulations in vivo in the FSaIIC murine fibrosarcoma," *Cancer*

Res., vol. 50, no. 11, pp. 3339–3344, 1990.

[51] B. A. Teicher, J. S. Lazo, and A. C. Sartorelli, "Classification of antineoplastic agents by their selective toxicities toward oxygenated and hypoxic tumor cells," *Cancer Res.*, vol. 41, no. 1, pp. 73–81, 1981.

[52] S. Koch, F. Mayer, F. Honecker, M. Schittenhelm, and C. Bokemeyer, "Efficacy of cytotoxic agents used in the treatment of testicular germ cell tumours under normoxic and hypoxic conditions in vitro," *Br. J. Cancer*, vol. 89, no. 11, pp. 2133–2139, 2003.

[53] L. H. Gray, A. Conger, M. Ebert, S. Hornsey, and O. C. A. Scott, "The concentration of oxygen dissolved in tissues at the time of irradiation as a factor in radiotherapy," *Br. J. Radiol.*, vol. 26, no. 312, pp. 638–648, 1953.

[54] D. Ewing, "The oxygen fixation hypothesis: a reevaluation," *Am. J. Clin. Oncol.*, vol. 21, no. 4, pp. 355–361, 1998.

[55] H. Ahsan, A. Ali, and R. Ali, "Oxygen free radicals and systemic autoimmunity," *Clin. Exp. Immunol.*, vol. 131, no. 3, pp. 398–404, 2003.

[56] D. R. Grimes and M. Partridge, "A mechanistic investigation of the oxygen fixation hypothesis and oxygen enhancement ratio," *Biomed. Phys. Eng. express*, vol. 1, no. 4, p. 45209, 2015.

[57] M. Valko, M. Izakovic, M. Mazur, C. J. Rhodes, and J. Telser, "Role of oxygen radicals in DNA damage and cancer incidence," *Mol. Cell. Biochem.*, vol. 266, no. 1–2, pp. 37–56, 2004.

[58] K. J. A. Davies, "Protein modification by oxidants and the role of proteolytic enzymes," *Biochem. Soc. Trans.*, vol. 21, no. 2, pp. 346–353, 1993.

[59] T. Lindahl, "Instability and decay of the primary structure of DNA," *Nature*, vol. 362, no. 6422, pp. 709–715, 1993.

[60] B. Haliwell, "Free radicals antioxidants and human disease: curiosity, cause or consequence," *Lancet*, vol. 344, no. 7, pp. 21–724, 1994.

[61] D. Dreher and A. F. Junod, “Role of oxygen free radicals in cancer development,” *Eur. J. Cancer*, vol. 32, no. 1, pp. 30–38, 1996.

[62] P. S. Brookes, A.-L. Levonen, S. Shiva, P. Sarti, and V. M. Darley-Usmar, “Mitochondria: regulators of signal transduction by reactive oxygen and nitrogen species 1, 2,” *Free Radic. Biol. Med.*, vol. 33, no. 6, pp. 755–764, 2002.

[63] B. A. Freeman and J. D. Crapo, “Biology of disease: free radicals and tissue injury.,” *Lab. Invest.*, vol. 47, no. 5, pp. 412–426, 1982.

[64] L. Y. Lu, N. Ou, and Q.-B. Lu, “Antioxidant induces DNA damage, cell death and mutagenicity in human lung and skin normal cells,” *Sci. Rep.*, vol. 3, 2013.

[65] Y. Liu, G. Fiskum, and D. Schubert, “Generation of reactive oxygen species by the mitochondrial electron transport chain,” *J. Neurochem.*, vol. 80, no. 5, pp. 780–787, 2002.

[66] T.-T. Huang, Y. Zou, and R. Corniola, “Oxidative stress and adult neurogenesis—effects of radiation and superoxide dismutase deficiency,” in *Seminars in cell & developmental biology*, 2012, vol. 23, no. 7, pp. 738–744.

[67] W. A. Pryor, “Oxy-radicals and related species: their formation, lifetimes, and reactions,” *Annu. Rev. Physiol.*, vol. 48, no. 1, pp. 657–667, 1986.

[68] I. Fridovich, “Superoxide anion radical (O· 2), superoxide dismutases, and related matters,” *J. Biol. Chem.*, vol. 272, no. 30, pp. 18515–18517, 1997.

[69] Q.-B. Lu, Q.-R. Zhang, N. Ou, C.-R. Wang, and J. Warrington, “In vitro and in vivo studies of non-platinum-based halogenated compounds as potent antitumor agents for natural targeted chemotherapy of cancers,” *EBioMedicine*, vol. 2, no. 6, pp. 544–553, 2015.

[70] Q.-B. Lu, *New theories and predictions on the ozone hole and climate change*. World Scientific, 2015.

[71] P. A. Jeggo and M. Löbrich, “How cancer cells hijack DNA double-strand break

repair pathways to gain genomic instability," *Biochem. J.*, vol. 471, no. 1, pp. 1–11, 2015.

[72] O. V Belov, E. A. Krasavin, M. S. Lyashko, M. Batmunkh, and N. H. Sweilam, "A quantitative model of the major pathways for radiation-induced DNA double-strand break repair," *J. Theor. Biol.*, vol. 366, pp. 115–130, 2015.

[73] C. Negritto, "Repairing double-strand DNA breaks," *Nat. Educ.*, vol. 3, no. 9, p. 26, 2010.

[74] T. K. Kelly, T. B. Miranda, G. Liang, B. P. Berman, J. C. Lin, A. Tanay, and P. A. Jones, "H2A. Z maintenance during mitosis reveals nucleosome shifting on mitotically silenced genes," *Mol. Cell*, vol. 39, no. 6, pp. 901–911, 2010.

[75] A. Dupré, L. Boyer-Chatenet, and J. Gautier, "Two-step activation of ATM by DNA and the Mre11–Rad50–Nbs1 complex," *Nat. Struct. Mol. Biol.*, vol. 13, no. 5, pp. 451–457, 2006.

[76] O. A. Sedelnikova, E. P. Rogakou, I. G. Panyutin, and W. M. Bonner, "Quantitative detection of 125IdU-induced DNA double-strand breaks with γ-H2AX antibody," *Radiat. Res.*, vol. 158, no. 4, pp. 486–492, 2002.

[77] M. Podhorecka, A. Skladanowski, and P. Bozko, "H2AX phosphorylation: its role in DNA damage response and cancer therapy," *J. Nucleic Acids*, vol. 2010, 2010.

[78] L. J. Kuo and L.-X. Yang, "γ-H2AX-a novel biomarker for DNA double-strand breaks," *In Vivo (Brooklyn).*, vol. 22, no. 3, pp. 305–309, 2008.

[79] R. Wang, F. Jin, and H. Zhong, "A novel experimental hypoxia chamber for cell culture," *Am. J. Cancer Res.*, vol. 4, no. 1, p. 53, 2014.

[80] S. M. Bakmiwewa, B. Heng, G. J. Guillemin, H. J. Ball, and N. H. Hunt, "An effective, low-cost method for achieving and maintaining hypoxia during cell culture studies," *Biotechniques*, vol. 59, no. 4, pp. 223–229, 2015.

[81] R. E. Ellis, J. Yuan, and H. R. Horvitz, "Mechanisms and functions of cell death,"

Annu. Rev. Cell Biol., vol. 7, no. 1, pp. 663–698, 1991.

[82] H. Steller, "Mechanisms and genes of cellular suicide," *Science (80-.).*, vol. 267, no. 5203, p. 1445, 1995.

[83] S. Nagata, "Apoptosis by death factor," *Cell*, vol. 88, no. 3, pp. 355–365, 1997.

[84] S. Rathore, G. Datta, I. Kaur, P. Malhotra, and A. Mohmmed, "Disruption of cellular homeostasis induces organelle stress and triggers apoptosis like cell-death pathways in malaria parasite," *Cell Death Dis.*, vol. 6, no. 7, p. e1803, 2015.

[85] S. W. Lowe and A. W. Lin, "Apoptosis in cancer," *Carcinogenesis*, vol. 21, no. 3, pp. 485–495, 2000.

[86] C. Stadelmann, T. L. Deckwerth, A. Srinivasan, C. Bancher, W. Brück, K. Jellinger, and H. Lassmann, "Activation of caspase-3 in single neurons and autophagic granules of granulovacuolar degeneration in Alzheimer's disease: evidence for apoptotic cell death," *Am. J. Pathol.*, vol. 155, no. 5, pp. 1459–1466, 1999.

[87] M. E. Guicciardi and G. J. Gores, "Life and death by death receptors," *FASEB J.*, vol. 23, no. 6, pp. 1625–1637, 2009.

[88] N. Özören and W. S. El-Deiry, "Cell surface death receptor signaling in normal and cancer cells," in *Seminars in cancer biology*, 2003, vol. 13, no. 2, pp. 135–147.

[89] S. Kothakota, T. Azuma, C. Reinhard, A. Klippel, J. Tang, K. Chu, T. J. McGarry, M. W. Kirschner, K. Koths, and D. J. Kwiatkowski, "Caspase-3-generated fragment of gelsolin: effector of morphological change in apoptosis," *Science (80-.).*, vol. 278, no. 5336, pp. 294–298, 1997.

[90] K. Buch, T. Peters, T. Nawroth, M. Sänger, H. Schmidberger, and P. Langguth, "Determination of cell survival after irradiation via clonogenic assay versus multiple MTT Assay-A comparative study," *Radiat. Oncol.*, vol. 7, no. 1, p. 1, 2012.

[91] N. A. P. Franken, H. M. Rodermond, J. Stap, J. Haveman, and C. Van Bree, "Clonogenic assay of cells in vitro," *Nat. Protoc.*, vol. 1, no. 5, pp. 2315–2319, 2006.

[92] J. C. Stockert, A. Blázquez-Castro, M. Cañete, R. W. Horobin, and Á. Villanueva, "MTT assay for cell viability: Intracellular localization of the formazan product is in lipid droplets," *Acta Histochem.*, vol. 114, no. 8, pp. 785–796, 2012.